Environmental Microbiology
April 2015, Volume 17, Issue 4, Pages 1152-1165
http://dx.doi.org/10.1111/1462-2920.12535

Outer membrane vesicles are vehicles for the delivery of *Vibrio tasmaniensis* virulence factors to oyster immune cells

Audrey Sophie Vanhove[1,2,3,4], Marylise Duperthuy[2,5], Guillaume M. Charrière[1,2,3,4], Frédérique Le Roux[6,7,8], David Goudenège[6,7,8], Benjamin Gourbal[9], Sylvie Kieffer-Jaquinod[10,11,12], Yohann Couté[10,11,12], Sun Nyunt Wai[5] and Delphine Destoumieux-Garzón[1,2,3,4,*]

[1] Ecology of Coastal Marine Systems, CNRS UMR 5119, Montpellier, France
[2] Ecology of Coastal Marine Systems, Ifremer, Montpellier, France
[3] Ecology of Coastal Marine Systems, University of Montpellier 1, Montpellier, France
[4] Ecology of Coastal Marine Systems, University of Montpellier 2 and IRD, Montpellier, France
[5] Department of Molecular Biology, The Laboratory for Molecular Infection Medicine Sweden (MIMS), Umeå University, Umeå, Sweden
[6] Unité Physiologie Fonctionnelle des Organismes Marins, Ifremer, Plouzané, France
[7] Integrative Biology of Marine Models UPMC Univ Paris 06, Sorbonne Universités, Roscoff Cedex, France
[8] Integrative Biology of Marine Models, CNRS UMR 8227, Station Biologique de Roscoff, Roscoff Cedex, France
[9] Ecology and Evolution of Interactions, CNRS UMR 5244, Université de Perpignan Via Domitia, Perpignan Cedex, France
[10] U1038, Université Grenoble-Alpes, Grenoble, France
[11] iRTSV, Biologie à Grande Echelle, CEA, Grenoble, France
[12] U1038, INSERM, Grenoble, France

*: Corresponding author : Delphine Destoumieux-Garzón, tel. (+33) 467 14 46 25 ; Fax (+33) 467 14 46 22 ; email address : ddestoum@univ-montp2.fr

Abstract:

Vibrio tasmaniensis LGP32, a facultative intracellular pathogen of oyster haemocytes, was shown here to release outer membrane vesicles (OMVs) both in the extracellular milieu and inside haemocytes. Intracellular release of OMVs occurred inside phagosomes of intact haemocytes having phagocytosed few vibrios as well as in damaged haemocytes containing large vacuoles heavily loaded with LGP32. The OMV proteome of LGP32 was shown to be rich in hydrolases (25%) including potential virulence factors such as proteases, lipases, phospholipases, haemolysins and nucleases. One major caseinase/gelatinase named Vsp for vesicular serine protease was found to be specifically secreted through OMVs in which it is enclosed. Vsp was shown to participate in the virulence phenotype of LGP32 in oyster experimental infections. Finally, OMVs were highly protective against antimicrobial peptides, increasing the minimal inhibitory concentration of polymyxin B by 16-fold. Protection was conferred by OMV titration of polymyxin B but did not depend on the activity of Vsp or another OMV-associated protease. Altogether, our results show that OMVs contribute to the pathogenesis of LGP32, being able to deliver virulence factors to host immune cells and conferring protection against antimicrobial peptides.

Introduction

Characterizing the molecular bases of vibrio-host interactions is of prime importance to understand how colonization is orchestrated and persistence established (Kremer et al., 2013) (Lindell et al., 2012). Oysters are naturally colonized by pathogenic and non-pathogenic vibrios but attention has mainly been paid to pathogenic interactions. Pathogenic strains related to *Vibrio aestuarianus* or *Vibrio splendidus* have been repeatedly isolated during massive mortalities of *Crassostrea gigas* (for review see (Schmitt et al., 2011). Strains of *V. aestuarianus* have evolved a so-called "outsider strategy" to promote an extracellular life cycle within the oyster by interacting specifically with oyster hemocytes (Olivot et al., 2006). Indeed, the hemocytes of oysters infected with the *V. aestuarianus* strain 01/32 displayed lower adhesion and phagocytosis capacities as well as increased production of ROS (Labreuche et al., 2006; Labreuche et al., 2010). On the contrary, the strain LGP32 (Gay et al., 2004) recently assigned to *V. tasmaniensis* within the Splendidus clade (Sawabe et al., 2013) was found to be a facultative intracellular pathogen that invades the oyster immune cells, the hemocytes, in which it inhibits phagosome maturation and ROS production (Duperthuy et al., 2011). An *ompU*-deletion mutant deficient for cell invasion was shown to be impaired in virulence, suggesting that cell invasion is required for virulence of LGP32. While mechanisms of cell invasion have been described in details, the intracellular lifestyle (intravacuolar/intracytosolic) of LGP32 remains unknown and the molecular bases of its intracellular survival and virulence are still poorly understood (Duperthuy et al., 2011).

Secretion of extracellular products (ECPs) is the major mechanism by which Gram-negative pathogens communicate with and intoxicate host cells (Kuehn and Kesty, 2005). ECPs of vibrios pathogenic for marine animals have been described for their content in toxins. Among them, molecules with haemolytic, cytolytic, proteolytic and lipolytic activities have been identified (for review see (Méndez et al., 2012), a major attention being paid to extracellular proteolytic enzymes. Those toxic compounds required for the life cycle of microorganism are secreted by both non-pathogenic and pathogenic microorganisms. They can be lethal to the host when produced by pathogenic bacteria (Miyoshi and Shinoda, 2000). Thus, metalloproteases are important virulence factors in a broad series of human and animal diseases (Shinoda and Miyoshi, 2011). In the *V. astuarianus* strain 01/32, ECPs were found to mediate avoidance of phagocytosis (Labreuche et al., 2006a), to cause major damages to hemocyte *in vitro* (Labreuche et al., 2010) and to be toxic for oysters (Labreuche et al., 2006b). This toxicity would be conferred by the Vam metalloprotease (Labreuche et al., 2010). Similarly, in *V. tasmaniensis* LGP32, the Vsm metalloprotease was found to be the main toxic factor of ECPs (Le Roux et al., 2007) while the contribution of the InhA/PrtV

protease was minor (Binesse et al., 2008). Still, the major metalloprotease Vsm was not required for virulence in experimental infections (Le Roux et al., 2007).

ECPs have been shown to contain insoluble vesicles released from the envelope of bacteria (Deatherage et al., 2009). Outer membrane vesicles (OMVs), which form the insoluble fraction of Gram-negative bacteria ECPs, are extruded from the bacterial cell surface and may entrap some of the underlying periplasmic contents (Wai et al., 1995; Beveridge, 1999). They are actually considered as a novel secretion system in Gram-negative bacteria (Lee et al., 2008). OMVs can perform a variety of functions, including binding and delivery of DNA, transport of virulence factors, protection of the cell from outer membrane targeting antimicrobials and ridding the cell of toxic envelope proteins (Manning and Kuehn, 2013). Thus, they are major players in the interaction between Gram-negative bacteria and both the prokaryotic and eukaryotic cells in their environment (Kulp and Kuehn, 2010). By their transport and protective functions, they play an essential role in host-pathogen interactions (Kuehn and Kesty, 2005).

OMVs, which benefit from a small size, adhesive properties, and ability to carry and deliver toxic components into host cells, have been proposed to play a significant role in the dissemination and delivery of virulence factors for Gram-negative pathogens (Ellis and Kuehn, 2010). The human pathogens *V. cholerae, V. vulnificus* and the fish pathogen *V. anguillarum* are known to actively secrete OMVs during their growth (Chatterjee and Das, 1967; Hong et al., 2009; Kim et al., 2010). In several vibrio species, virulence factors have been proposed to be associated with such OMVs (Boardman et al., 2007; Kim et al., 2010). In addition, the release of OMVs by Gram-negative bacteria has recently been shown be protective against bacteriophages and antimicrobial peptides (AMPs) (Manning and Kuehn, 2011; Duperthuy et al., 2013). AMPs from both eukaryotic and prokaryotic origin have been evidenced in oyster hemolymph. Indeed, not only do hemocytes produce a broad series of endogenous AMPs (for review (Schmitt et al., 2012) but bacteriocin-like peptides are present in oyster plasma (Defer et al., 2013). To date little is known on the effectors of AMP-resistance in oyster pathogenic vibrios (Duperthuy et al., 2010) and the potential role of OMVs remains unexplored. While global proteomic studies of native OMVs are required to elucidate the functions of OMVs (Lee et al., 2008), global descriptions of OMV proteomes remain very scarce in *Vibrio* species.

Here we asked whether *V. tasmaniensis* LGP32 produces OMVs and how they are involved in pathogenesis by focusing on the delivery of virulence factors and the protection against AMPs. To this aim, we isolated OMVs from LGP32 ECPs, developed a global proteomic characterization of LGP32 OMVs and studied the interaction of OMVs with the oyster immune cells. Our results show that LGP32 secretes OMVs rich in hydrolases which can be internalized by host immune cells or be

released by intraphagosomal bacteria. Among the encapsulated hydrolases, one major gelatinase/caseinase named Vsp (VS_II0815) for vesicular serine protease was found to be specifically secreted through OMV production. Vsp was shown here to participate in the virulence phenotype of LGP32 in oyster experimental infections. Besides, OMVs were shown to be protective against antimicrobial peptides independently of Vsp activity.

Results

The strain LGP32 secretes outer membrane vesicles

Vesicle production by LGP32 was first examined by electron microscopy. Logarithmic phase cultures of LGP32 showed the release of small vesicles with an average diameter of 30 to 50 nm, as revealed by negative staining. Vesicles were observed both in the culture medium and bound to the bacterial membrane and polar flagellum (Fig. 1A-E). Extracellular products (ECPs) were separated from *Vibrio* cells by centrifugation and filtration (0.2 µm). They were further ultracentrifuged to separate vesicles from soluble products. The isolated vesicles were intact and homogeneous as observed after negative staining by transmission electron microscopy (Fig. 1F). Their diameter ranged from 30 and 50 nm, consistent with the size observed before vesicle purification. The protein concentration of the vesicles released by LGP32 in Zobell medium was measured at 1 µg mL^{-1}.

The protein composition of the purified vesicles was determined by a proteomic approach consisting in stacking electrophoresis followed by trypsin digestion and LC-MS/MS sequencing. Two OMV preparations were analyzed. The first preparation (OMV prep #1) corresponded to crude OMVs while the second preparation obtained independently (OMV prep #2), was further purified by density gradient. Protein identification was achieved using Mascot and sequences obtained from the LGP32 genome (Le Roux et al., 2009). Only proteins identified by more than 3 peptides were kept for further analysis. A total of 188 and 177 vesicle-associated proteins were identified in the OMV prep #1 and #2, respectively (Table S1). Only the 132 proteins common to both preparations were considered to belong to the OMV proteome. A subcellular localization could be assigned to most of them (98.5%). Consistent with the composition expected for outer membrane vesicles (OMVs), Tat and Sec-exported proteins, outer membrane and periplasmic proteins accounted for 88.6% of the identified proteins (Table S1). Most of the remaining proteins were identified as extracellular flagellar proteins (6.8%) (Table S2).

OMVs of LGP32 display a high content in proteases

Among the proteins identified, a large fraction (33 proteins, 25%) encoded enzymes such as proteases, sulfatases, phosphatases, nucleases and lipases (Table S1). We focused here on proteases,

which can be important virulence factors in vibrios. Putative proteases are also the most abundant hydrolases found in our OMV proteomic analysis (15 proteins, 45.5% of the identified hydrolases, 11.4% of the identified proteins, Table S1). We asked whether such proteases were enclosed within OMVs. Intact OMVs (2 mg ml^{-1}) displayed little to no proteolytic activity when tested in the azocasein assay (Fig. 2A). This contrasted strongly with the soluble products of LGP32 ECPs (supernatant of ultracentrifuged ECPs), which displayed strong proteolytic activity at 1 mg ml^{-1} mainly due to the Vsm protease (Fig. 2A, Fig. S1). Interestingly, when OMVs were lysed by treatment with 0.1% triton X-100 (Fig. 2C), major protease activity was detected (Fig. 2A), showing that proteases enclosed within OMVs were released upon membrane disruption.

A putative serine protease (VS_II0815) is the major gelatinase/caseinase of OMVs

To identify the OMV-associated protease(s), OMVs were subjected to zymography on both a casein- and a gelatin-containing polyacrylamide gel. On both substrates, one protease band was observed at an approximate molecular mass of 30 kDa (Fig. 2B). The same band was observed for OMVs from wild-type or *Δvsm* LGP32 (Fig. S1) showing that this protease activity is not related to the *vsm* gene. Consistent with an intravesicular localization of the protease, no protease band at the same size was observed in supernatant depleted of OMVs (Fig. S1). The gelatinase activity was similar at 20°C and 37°C, and stable in a pH range of 5.6 to 7.7 (Fig. S2). The protease evidenced by zymography was identified by trypsin in-gel digestion followed by MS-MS sequencing. A total of 6 peptides identified the protein (23% coverage), all of which aligned with the central-most region of the VS_II0815 sequence (Fig. 3), a putative S1 family secreted trypsin-like serine protease (calculated mass 39 kDa). The Vesicular Serine Protease (Vsp) isolated from OMVs was 47.5 % identical to the VesA serine protease of *V. cholerae* VCA0803 (Fig. 3).

To confirm that Vsp is the main gelatinase/caseinase observed on zymography of LGP32 OMVs, we constructed an isogenic deletion mutant. The LGP32 *Δvsp* mutant did not display any growth defect in Zobell growth medium nor in oyster plasma (Fig. S3A). We then compared the gelatin zymogram profile of OMVs obtained from the wild-type and *Δvsp* mutant. Upon *vsp* deletion, the active band assigned to Vsp disappeared from the zymography (Fig. 2B). Altogether, our data show that Vsp (VS_II0815 gene product) is the major gelatinase/caseinase of LGP32 OMVs.

The virulence of the Δ*vsp* mutant is attenuated in oyster experimental infections

To determine whether Vsp could contribute to the virulence of LGP32, juvenile oysters were infected with the wild-type LGP32 or the *Δvsp* isogenic mutant. In two independent experiments, groups of 45 oysters received an injection of 4×10^7 CFU of each strain. No mortalities were recorded over 7 days for control oysters injected with sterile seawater. Interestingly, the *Δvsp* mutant was significantly

impaired in terms of virulence compared to the wild-type LGP32 as revealed by Kaplan-Meier survival curves (P = 0.0004, log-rank test). Indeed, oyster mortalities at day 7 were reduced from 91.2% for the wild-type LGP32 to 55.7% for the *Δvsp* isogenic mutant (Fig. 4). Because *in vivo* complementation of the virulence phenotype could not be achieved due to the toxicity of the *vsp* gene product for the *Escherichia coli* donor strain, we tested two additional Δ*vsp* mutants obtained independently in experimental infections. The Kaplan-Meir survival curves showed a significant attenuated phenotype for both mutants (P = 0.027 and P = 0.006) (Fig. S5). Consequently, it is very unlikely that the attenuated phenotype associated to the Δ*vsp* deletion is due to a second site mutation. We concluded that the Δ*vsp* deletion attenuates LGP32 virulence in oyster experimental infections.

<u>OMVs can be delivered to host immune cells both intracellularly and extracellularly</u>

The presence of Vsp inside OMVs prompted us to investigate the role of OMVs in the delivery of virulence factors to host cells in the course of LGP32 infectious process. We first asked whether OMVs could be secreted inside hemocytes during its intracellular stages. Hemocytes having phagocytosed LGP32 (30 min-contact) were therefore observed by transmission electron microscopy. Vibrios were found inside phagosomes without any sign of bacterial cell envelope destruction nor lysis (Fig. 5A-D). When hemocytes contained only few vibrios, vibrios were observed as single cells inside phagosomes without evident hemocyte damage (Fig. 5A). When hemocytes were invaded by abundant vibrios (Fig. 5C&D), one to four vibrios were present inside large vacuoles and hemocytes displayed important cytoplasmic disorders with (i) a loss of integrity of intracellular organelles including endoplasmic reticulum and mitochondria and (ii) an accumulation of vacuoles of heterogeneous sizes. No vibrios were observed in the cytoplasm of hemocytes outside phagosomes but some vacuoles containing vibrios displayed membrane disruptions and cytoplasmic disorders. Damages to the hemocyte cytoplasmic membrane were also observed (Fig. 5D). Importantly, for the vast majority of infected hemocytes, vesicles of 30-50 nm diameter reminiscent of those observed in LGP32 culture medium were visible releasing from the bacterial membrane or free inside phagosomes (Fig. 5B&D). We then asked whether such OMVs, which are also released extracellularly (Fig. 1), could enter host cells. For that, OMVs fluorescently labeled with PKH26 were incubated with hemocytes for 2 h. A strong red fluorescent signal was observed by confocal microscopy within hemocytes (Fig. 5E&F), indicating that OMVs were internalized upon contact with hemocytes.

<u>OMVs confer protection against antimicrobial peptides independently of Vsp</u>

We then asked whether OMV production could confer protection against the antimicrobial peptides (AMPs) found in oyster plasma. Indeed, a remarkable stimulation of OMV production was observed

by electron microscopy when LGP32 was cultured in oyster plasma (Fig. S3C). To test the protective effect of OMVs, LGP32 was exposed to a membrane-active AMP, Polymyxin B (PmB) in the presence of OMVs isolated from the wild-type or the Δ*vsp* mutant. A dose-dependent protective effect of LGP32 OMVs was observed against PmB, whose minimal inhibitory concentration (MIC = 0.78 µM) increased by 2-fold in the presence of 6.25 µg ml^{-1} OMVs (protein concentration) and up to 16-fold in the presence of 50 µg ml^{-1} OMVs (Table 1). The same protection was obtained with 50 µg ml^{-1} OMVs from the Δ*vsp* mutant (Table 1). In addition, the MIC of PmB against the wild-type or the Δ*vsp* mutant were identical at 0.78 µM. Altogether, this indicates that OMVs provide a significant and dose-dependent protection against AMPs independently of *vsp* expression.

To determine whether the OMV-mediated protection could be conferred by enclosed proteases other than Vsp, we incubated PmB with wild-type OMVs for 6 h and monitored the PmB trace by reversed phase HPLC and SDS-PAGE. No difference in the intensity of the PmB band was observed by SDS-PAGE, indicating that PmB is not degraded by intravesicular proteases (Fig. 6A). However, the HPLC absorbance peak corresponding to PmB disappeared from the chromatogram over the time course of the incubation, indicating that at least PmB binds to OMVs (Fig. 6B). Altogether, our data indicate that PmB is not degraded but rather titrated by OMVs.

Discussion

Results showed that *V. tasmaniensis* strain LGP32 releases outer membrane vesicles (OMVs) containing virulence factor(s) which can be delivered to host immune cells either intracellularly or extracellularly. A total of 132 proteins identified by at least 3 peptides were found associated to LGP32 OMVs (Table S1). In other bacterial species, 44 to 236 OMV-associated proteins were identified depending on the techniques used for proteomics (Lee et al., 2008). Most of the LGP32 OMV proteins were predicted to be Tat or Sec exported, to localize at the periplasm or at the outer-membrane (88.6 %) (Table S1). This composition is consistent with the biogenesis of Gram-negative OMVs (Deatherage et al., 2009; Kulp and Kuehn, 2010). Besides, 7.6 % of the proteins were predicted to be extracellular. Among them, 6.8 % were flagellar proteins suggesting the presence of non-observed contaminating flagella. Surprisingly, flagellar proteins were still found when OMVs were purified by density gradient (Table S1). The observation of vesicles intimately associated with the flagellum by electron microscopy (Fig. 1C-E) suggests that OMVs can be released from the LGP32 flagella sheath as also observed in *Vibrio fisheri* (Brennan et al., 2014). In *V. cholerae*, the flagella sheath was shown to be composed of the outer membrane, containing lipopolysaccharide (Fuerst and Perry, 1988) and outer membrane proteins (Bari et al., 2012). Interestingly, a recent study showed that OMVs from *E. coli* contain flagellar proteins (Manabe et al., 2013). It is therefore likely that the OMVs obtained from LGP32 contain both periplasmic and flagellar proteins as a result of

different sites of biogenesis. Finally, 2.3 % of the proteins were predicted to localize at the inner membrane. Such observations have also been made in other species, in which cytoplasmic and inner membrane potential virulence factors were found to be components of OMVs (for review see (Lee et al., 2008).

One major function characterizing the OMV proteome of LGP32 was enzymatic activities (25 %). We indeed found several proteases, lipases, phospholipases, nucleases, hemolysins, and murein hydrolases associated to OMVs, as revealed by MS-MS sequencing. Together with siderophores and adhesins/invasins, also found associated to LGP32 OMVs (Table S1), these hydrolases correspond to potential virulence factors described in pathogenic *Vibrio* species (Zhang and Austin, 2005; Méndez et al., 2012). Their association with OMVs is in agreement with the protease, phospholipase, and hemolysin activities associated to OMVs of *V. anguillarum*, another pathogen for marine cultured species (Hong et al., 2009). Besides, consistent with the biogenesis and composition of OMVs, membrane transport (40.9 %) and cell wall/membrane biogenesis (13.6 %) were important functions associated to LGP32 OMV proteins. Indeed, we evidenced here many integral outer membrane proteins such as porins including the adhesin/invasin OmpU (Duperthuy et al., 2011), metal-siderophore transporters, ABC-transporters, efflux pumps, peptidoglycan-associated lipoproteins (Table S1). Altogether, molecular functions associated to LGP32 OMVs are similar to those found in OMVs from bacterial species other than vibrios (*e.g. Escherichia coli, Neisseria meningitis, Pseudomonas antartica*), which also display a large percentage of transport proteins (porins, ABC transporters), adhesins/invasins, but also hydrolases including potential virulence factors (proteases, hemolysins, murein hydrolases) and motility-related proteins (flagellins) (for review see (Lee et al., 2008)).

One important finding from this study is that OMVs can be delivered to host cells both intracellularly, inside phagosomes, and extracellularly, by internalization (Fig. 5). From our electron microscopy data, intracellular release of OMVs could be part of LGP32 infectious process. Indeed we observed several vesicles attached to the bacteria as well as free vesicles of the same size (30-50 nm) inside the phagosome (Fig. 5B&D), which are likely released by the phagocytosed bacteria. Such vesicles were observed at early stages when few vibrios are present inside intact hemocytes but also at late stages, when multiple vibrios are observed inside large vacuoles of damaged hemocytes (Fig. 5A-D). The absence of cytosolic vibrios in invaded hemocytes clearly showed that LGP32 behaves as an intravacuolar pathogen. Interestingly, in *Legionella pneumophila*, a facultative intracellular pathogen replicating inside vacuoles of macrophages, intracellular release of OMVs was also observed, OMVs being found to inhibit the fusion of phagosomes with lysosomes (Fernandez-Moreira et al., 2006).

Since we earlier showed that LGP32 inhibits phagosome maturation (Duperthuy et al., 2011), one can hypothesize that, as in *L. pneumophila*, OMV release participates in the intracellular survival of LGP32. It can also be hypothesized that OMVs of LGP32 are vehicles for the delivery of candidate virulence factors to oyster immune cells (Fig. 5). Indeed, the OMV-mediated extracellular delivery of virulence factors to host cells has been reported in *A. actinomycetemcomitans* and *V. cholerae* (Chatterjee and Chaudhuri, 2011; Rompikuntal et al., 2012).

By focusing on proteases, we showed that potential virulence factors are specifically enclosed within OMVs. Indeed, while low proteolytic activity was associated to intact OMVs, major activity was released upon triton-lysis of OMVs (Fig. 2A). The gelatinase/caseinase activity enclosed in LGP32 OMVs was attributed to the putative serine protease VS_II0815, as revealed by MS-MS sequencing of the active band (Fig. 3) and zymography of a Δ*vsp* deletion mutant (Fig 2B). Importantly, VS_II0815 was absent from the soluble fraction of LGP32 extracellular products, *i.e.* ultracentrifuged supernatant devoid of OMVs (Fig. S1), showing it is specifically secreted through OMV release. VS_II0815 was therefore termed Vsp for vesicular serine protease. To our knowledge, such a specific intravesicular secretion of proteases is shown here for the first time. These observations are consistent with the view that OMVs can be considered as a secretion system *per se* (Lee et al., 2008). Noteworthy, we also showed that the previously characterized Vsm (Le Roux et al., 2007) was extravesicular, its gelatinase/caseinase activity being dominant in the supernatants after ultracentrifugation of extracellular products but absent in OMVs (Fig. S1). Therefore, its identification by MS-MS sequencing (Table S1), which is a very sensitive technique, was attributed to its high abundance in the extracellular milieu, contaminating our OMV preparation.

The OMV-secreted Vsp protease was shown to be homologous to the VesA serine protease of *V. cholerae* (Sikora et al., 2011) (47.5% sequence identity). Like VesA, it carries the canonical catalytic triad His95-Asp149-Ser254 as well as 3 out of the 4 conserved disulfide bridges of serine proteases (Fig. 3). In addition to a 29-residue signal peptide at N-terminal position, Vsp displays a potential transmembrane domain at its C-terminus. Both features are conserved in VesA (Fig 3). This C-terminal transmembrane domain can either be a sorting signal or an inner membrane anchor. The lack of peptides identified by MS-MS at the N- and C-terminus of the Vsp protease as well as its apparent mass on a polyacrylamide gel electrophoresis (30 kDa), lower than its calculated mass (39 kDa), strongly suggest that the Vsp protein isolated from OMVs results from the post-translational maturation of a larger precursor. Taken together with its localization inside OMVs, this indicates that Vsp is likely addressed to the inner membrane through its signal peptide, retained at the inner membrane by its Gly335-Phe353 C-terminal inner membrane anchor and finally released into the

periplasmic space upon proteolytic maturation. Such maturation could occur at several sites between residues 280 and 335, in the region separating the serine protease domain of Vsp from its C-terminal anchor. Indeed two Arg residues recognized by trypsin-like serine proteases as well as a Lys-Arg and a Arg-Arg-Arg multibasic site recognized by kexin-like serine proteases (Kobayashi et al., 2009) are found in this region (Fig. 3). In *V. cholera*e, VesA was proposed to be transported through T2SS but could not be observed in ultracentrifuged culture supernatants (Sikora et al., 2011). Because VesA lacks the Lys-Arg and Arg-Arg-Arg multibasic sites found in the Vsp sequence (Fig. 3), it could be retained at the inner membrane of *V. cholerae*.

Importantly, the virulence of three Δ*vsp* mutants was shown to be attenuated compared to the wild-type LGP32 in oyster experimental infections (Fig. 4 & S5). Therefore, we concluded that like other proteases involved in host-*Vibrio* pathogenic interactions (Shinoda and Miyoshi, 2011), the serine protease Vsp participates in the virulence phenotype of LGP32. This demonstrates that the OMV-mediated delivery of virulence factors contributes to LGP32 pathogenesis. Remarkably, unlike Vsp, the major metalloprotease Vsm, which was shown here to be extravesicular (Fig. S1), did not significantly modify the virulence status of LGP32 in experimental infections (Le Roux et al., 2007). It is still unknown at what stage of the pathogenesis Vsp is involved. Indeed, the Δ*vsp* deletion mutants did not show any evident phenotype on hemocyte primary cultures (data not shown), suggesting that Vsp does not have a direct effect on oyster hemocytes. Thus, the major phenotype observed in oyster experimental infections could rely on Vsp-dependent virulence factors expressed *in vivo*. For instance, Vsp could be required for the proteolytic actvation of LGP32 virulence factors as demonstrated for its homologue VesA from *Vibrio cholerae*, which activates the CtxA cholera toxin by proteolytic cleavage (Sikora et al., 2011).

Besides Vsp, potential virulence factors associated to OMVs of LGP32 deserve further investigation to better understand the role of OMVs in pathogenesis. Two putative hemolysins and a phospholipase D (PLD) found in our proteomic data (Table S1) are of particular interest. These toxins are indeed known for their lytic properties on biological membranes, causing damage to erythrocytes and other cell types, such as leukocytes or neutrophils (for review see (Méndez et al., 2012). Phospholipases D (PLD) are involved in virulence of different bacteria. In the intracellular pathogen *Corynebacterium pseudotuberculosis*, secreted PLD can be lethal for neutrophils and macrophages in which it is expressed at high levels (Yozwiak and Songer, 1993; McKean et al., 2007). Hemolysins are the most widely distributed toxins among pathogenic vibrios (Zhang and Austin, 2005). In *Vibrio vulnificus*, expression of the cytolysin-hemolysin VvhA in response to low-iron concentrations results in erythrocytes lysis providing iron for bacterial growth and pathogenicity (Lee et al., 2013). VvhA was

shown to be delivered to mouse cells through OMV secretion (Kim et al., 2010). Therefore, it is tempting to speculate that secretion of cytolytic enzymes such as hemolysins and PLD through OMV release (Fig. 5B&D) participates in the disruption of vacuole and cytoplasmic membrane observed when high numbers of intracellular vibrios are present inside hemocytes (Fig. 5D). Future functional studies will help identifying how far such OMV-associated proteins participate in the virulence phenotype of LGP32.

Finally, OMVs from LGP32 were shown here to be highly protective against antimicrobial peptides, increasing the MIC of PmB from 2- to 16-fold at OMV concentrations ranging from 6.25 to 50 µg mL^{-1} (Table 1). We believe that such OMV concentrations can be reached in oyster plasma. Indeed, while OMV production was rather low in rich culture medium (1 µg mL^{-1}), it increased strongly in the presence of plasma (Fig S3). The role of proteases in resistance to antimicrobial peptides (AMPs) has been shown in several bacterial species (Nizet, 2006). However, OMV protection against AMPs was not conferred by Vsp since (i) sensitivity to PmB was similar for the wild-type and Δ*vsp* mutant (Table 1), (ii) OMVs from the wild-type and Δ*vsp* mutant were similarly protective against PmB (Table 1), and (iii) PmB was not degraded upon contact with OMVs (Fig. 6). Rather, we found that OMV protection relies on titration by OMVs, probably due to the membrane-insertion properties of PmB into biological membranes (Tomarelli et al., 1949). Recent data on *V. cholerae* showed that only OMVs carrying the biofilm-associated extracellular matrix protein Bap1 were protective against the human AMP LL-37, with an increase of MIC by 4 fold (Duperthuy et al., 2013). As in LGP32, protection resulted from trapping of LL-37 and did not require proteolytic degradation of LL-37. Therefore, while the molecular bases of AMP binding to OMVs appear to differ among *Vibrio* species, OMVs similarly protect vibrios from AMPs by forming a protective shield in which AMPs are entrapped. A similar protective role was also recently proposed for *E. coli* OMVs on which both bacteriocins (AMPs from prokaryotic origin) and bacteriophages were found to be adsorbed, thus contributing to bacterial defenses (Manning and Kuehn, 2011). Since AMPs are both produced by the oyster microbiota and oyster tissues (Schmitt et al., 2012; Defer et al., 2013), OMV production may confer a major advantage for vibrios to colonize oysters.

Experimental procedures

Bacterial strains and culture condition

Escherichia coli strains Π3813 and β3914 (Le Roux et al., 2007) were used for cloning and conjugation, respectively. *E. coli* strains were grown in Luria Bertani (LB) at 37°C (Difco). The *Vibrio* strains (Table S3) were grown at 20°C either in artificial seawater (0.6 M NaCl, 20 mM KCl, 5 mM MgSO4, 1.4 mM MgCl2) supplemented with 4 g l^{-1} bactopeptone and 1 g l^{-1} yeast extract (referred to as Zobell medium) or in LB supplemented with NaCl 0.5 M (LB-NaCl). Chloramphenicol was used at 12.5 µg ml^{-1}. Thymidine (dT) and diaminopimelate (DAP) were supplemented when necessary to a final concentration of 0.3mM. Induction of *ccdB* expression under the control of P_{BAD} promoter was achieved by the addition of 0.2% L-arabinose to the growth media and repressed by 1% D-glucose.

Vector construction and mutagenesis

The LGP32 *Δvsp* derivative was constructed by allelic exchange using the method described previously (Le Roux et al., 2007). Briefly, alleles carrying an internal deletion were generated *in vitro* using a two-step PCR construction method (Binesse et al., 2008) using primers 281112-1 to 4 (Table S3) and cloned into PSW7848T, a R6K γ-*ori*-based suicide vector that encodes the *ccdB* toxin gene under the control of an arabinose-inducible and glucose-repressible promoter, P_{BAD}. Matings between *E. coli* and *Vibrio* were performed at 30°C as described previously (Le Roux et al., 2007). Selection of the plasmid-borne drug marker resulted in integration of the entire plasmid in the chromosome by a single crossover. Elimination of the plasmid backbone resulting from a second recombination step was selected by arabinose induction of the *ccdB* toxin gene. Mutants were screened by PCR using primers 281112-1 and 4. *vsp* deletion was verified by sequencing using primers VS_II0815-Fw2 and VS_II0815-Rv2 (Table S3).

Extracellular products (ECPs) and Outer Membrane Vesicle (OMV) preparation

Bacterial ECP were produced by the cellophane overlay method described by (Liu, 1957). Briefly, 2 ml of stationary phase culture were spread onto a Zobell agar plate covered by a sterile cellophane film. After 48 h of incubation at 20°C, the cellophane overlay was transferred to an empty Petri dish. Cells were harvested in 250 µl of 0.1 M cold sodium-phosphate buffer (pH 7). Bacterial cells were removed by centrifugation at 16 000 *g* at 4°C for 30 min. The supernatant was filtered through a 0.22 µm-pore-size PVDF membrane filter (Millipore). OMVs were obtained from ECPs by ultracentrifugation at 100 000 *g* for 2 h at 4°C using a TLA110 rotor (Beckman Instruments Inc.). The ultracentrifuged supernatant (Sn) was kept at -20°C while crude OMVs were washed with 0.1 M cold sodium-phosphate buffer (pH7) and suspended in cold phosphate buffer saline (PBS) (Wai et al., 2003). When

OMVs were purified by density gradient centrifugation, Optiprep gradient was used as described previously (Balsalobre et al., 2006). Briefly, crude OMVs preparations suspended in PBS buffer were added on the top of gradient layers and centrifuged at 100 000 *g* for 3 h at 4°C. Fractions of 200 µl were sequentially collected from the top of the ultracentrifugation tube and analyzed by SDS-PAGE and immunoblotting using anti-OmpU antiserum to identify the fractions containing OMVs. The OMVs protein concentration was determined by the Bradford method with Micro-BCA protein assay reagent (Pierce Biotechnology, Rockford, IL, USA). OMVs were stored at -20°C until use.

Protease activity quantification

Protease activity of ECPs, intact or lysed OMVs, was determined using azocasein (Sigma A2765) as a substrate. When indicated, OMVs 2 mg ml^{-1} were lysed for 30 min at 20°C in PBS containing 0.1% Triton X-100 (Sigma T8787). Intact OMVs were kept in PBS. Then, 100 µl of azocasein (5 mg ml^{-1} in 100 mM Tris-HCl buffer, pH 8.5) were added to 50 µl of OMVs preparations. The mixture was incubated at 20°C for 1 h. The undigested substrate was precipitated by adding 100 µl of 10% trichloroacetic acid to the reaction mixture during 5 min on ice, followed by centrifugation at 12 000 *g* and 4°C for 5 min. The supernatant (100 µl) was neutralized by addition of an equal volume of 1 N NaOH. After mixing, the absorbance at 440 nm was determined (Tomarelli et al., 1949). Significance of differences was determined using a Student's *t* test.

Gelatin zymography

OMVs were analysed for protease activity by a gelatin substrate gel electrophoresis. 5 µg of OMVs resuspended in loading buffer (62.5 mM Tris HCl, pH 6.8, 4% SDS (w/v), 20% (v/v) glycerol, and 0.001% bromophenol blue) in the absence of reducing agents were loaded onto a 12.5% SDS-PAGE containing 0.2% gelatin. After electrophoresis, the gels were washed in renaturing buffer (50 mM Tris-HCl pH 7.6 and 2.5% Triton X-100) for 2 h at room temperature, and then incubated overnight at 37°C in the developing buffer (50 mM Tris-HCl pH 7.6, 200 mM NaCl, 5 mM $CaCl_2$, 0.02% w/v Brij 35). The gels were stained with a solution containing 0.1% Coomassie Brilliant Blue R-250. Formation of clear zone against the blue background on the polyacrylamide gels indicated the gelatinolytic activity (Binesse et al., 2008).

Proteomic and LC-MS/MS analyses

Protein preparation and digestion. OMV proteins solubilized in Laemmli buffer were stacked in the top of a 4-12% NuPAGE gel (Invitrogen) before R-250 Coomassie blue staining. The gel band was manually excised and cut in pieces before being washed by 6 successive incubations of 15 min in 25 mM NH_4HCO_3 and in 25 mM NH_4HCO_3 containing 50% (v/v) acetonitrile. Gel pieces were then

454 dehydrated with 100 % acetonitrile and incubated for 45 min at 53°C with 10 mM DTT in 25 mM
455 NH_4HCO_3 and for 35 min in the dark with 55 mM iodoacetamide in 25 mM NH_4HCO_3. Alkylation was
456 stopped by adding 10 mM DTT in 25 mM NH_4HCO_3 and mixing for 10 min. Gel pieces were then
457 washed again by incubation in 25 mM NH_4HCO_3 before dehydration with 100% acetonitrile. Modified
458 trypsin (Promega, sequencing grade) in 25 mM NH_4HCO_3 was added to the dehydrated gel pieces for
459 an overnight incubation at 37°C. Peptides were then extracted from gel pieces in three 15 min
460 sequential extraction steps in 30 µl of 50% acetonitrile, 30 µL of 5% formic acid and finally 30 µL of
461 100% acetonitrile. The pooled supernatants were then dried under vacuum.

462 *NANO-LC-MS/MS analyses.* The dried extracted peptides were resuspended in 5% acetonitrile and
463 0.1% trifluoroacetic acid and analysed by online nanoLC-MS/MS (Ultimate 3000, Dionex and LTQ-
464 Orbitrap Velos pro, Thermo Fischer Scientific). Peptides were sampled on a 300 µm x 5 mm PepMap
465 C18 precolumn and separated on a 75 µm x 250 mm C18 column (PepMap, Dionex). The nanoLC
466 method consisted in a 120 min-gradient at a flow rate of 300 nL min^{-1}, ranging from 5% to 37%
467 acetronitrile in 0.1% formic acid during 114 min before reaching 72% acetronitrile in 0.1% formic acid
468 for the last 6 min. MS and MS/MS data were acquired using Xcalibur (Thermo Fischer Scientific).
469 Spray voltage and heated capillary were respectively set at 1.4 kV and 200°C. Survey full-scan MS
470 spectra (m/z = 400–1600) were acquired in the Orbitrap with a resolution of 60 000 after
471 accumulation of 106 ions (maximum filling time: 500 ms). The twenty most intense ions from the
472 preview survey scan delivered by the Orbitrap were fragmented by collision induced dissociation
473 (collision energy 35%) in the LTQ after accumulation of 104 ions (maximum filling time: 100 ms).

474 *Bioinformatics analyses.* Data were processed automatically using Mascot Daemon software (version
475 2.3.2, Matrix Science). Concomitant searches against LGP32 and classical contaminant protein
476 sequence databases (4,500 sequences) and the corresponding reversed databases were performed
477 using Mascot (version 2.4). ESI-TRAP was chosen as the instrument, trypsin/P as the enzyme and 2
478 missed cleavage allowed. Precursor and fragment mass error tolerances were set respectively at 10
479 ppm and 0.6 Da. Peptide modifications allowed during the search were: carbamidomethyl (C, fixes)
480 acetyl (N-ter, variable), oxidation (M, variable) and deamidation (NQ, variable). The IRMa software
481 (Dupierris et al., 2009) was used to filter the results: conservation of rank 1 peptides, peptide
482 identification FDR < 1% (as calculated on peptide scores by employing the reverse database strategy),
483 and minimum of 3 specific peptide per identified protein group.

484 <u>Sequence annotation and subcellular localization</u>

485 Functional annotation of coding DNA sequences (CDSs) was manually assigned based on automated
486 annotation generated by the MicroScope platform pipeline (Vallenet et al., 2013) combined with
487 BlastP analysis, PFAM (Punta et al., 2012) and InterProScan search (Quevillon et al., 2005). Protein

subcellular localization (SCL) were predicted using a consensus-based approach that combine SCL tools results grouped by predicted features : SEC-dependent signal peptides was predicted using SignalP v4.0 (Petersen et al., 2011), PrediSi (Hiller et al., 2004) and Phobius v1.01 (Kall et al., 2004); twin-arginine (TAT) signal peptides using TatFind Server (Rose et al., 2002); lipoprotein signal peptides and membrane retention signal using LIPO (Berven et al., 2006), LipoP v1.0 (Rahman et al., 2008) and PRED-LIPO (Bagos et al., 2008); transmembrane alpha-helix (except signal peptide) of inner membrane protein using TMHMM v2.0 (Krogh et al., 2001), HMMTOP v2.0 (Tusnady and Simon, 2001) and Phobius v1.01 ; outer-membrane protein using HHomp (Remmert et al., 2009); and global prediction using PSORTb v3.0.2 (Yu et al., 2010), CELLO v2.5 (Yu et al., 2006) and SOSUIGramN (Imai et al., 2008). Enzymes were identified using the MEROPS database (Rawlings et al., 2012).

Experimental infection of oysters

Juvenile and adult diploid *Crassostrea gigas* were purchased from the Ifremer oyster hatchery in La Tremblade (Charente Maritime, France) and from a local oyster farm in Mèze (Gulf of Lion, France), respectively. Experimental infections were performed at 20 °C, as previously described (Duperthuy et al., 2010). Groups of 45 oysters were injected with wild-type or Δ*vsp* LGP32 (4 x 10^7 CFU per juvenile oyster or 2 x 10^8 CFU per adult oyster). Control animals were injected with an equal volume of sterile seawater (SSW). For every condition, oysters were placed for 24h in 3 separate tanks in 10 L of seawater (15 animals per tank). Mortalities were monitored daily over 7 days. The non-parametric Kaplan–Meier test was used to estimate Log-Rank values for comparing the survival curves (Kaplan and Meier, 1958). All experimental infections were performed according to the Ifremer animal care guideline and policy.

Observation of extracellular and intracellular OMVs by electron microscopy

For extracellular OMVs, logarithmic phase culture of LGP32 were negatively stained with 0.1% uranyl acetate and then placed on carbon-coated Formvar grids. To visualize intracellular OMVs, hemolymph was first collected from the pericardic cavity of oysters using a 2 mL syringe equipped with a 23-G needle. After counting, hemocytes were infected at a multiplicity of infection of 50:1 (30 min, room temperature) with stationary phase LGP32 previously opsonised with oyster plasma as described earlier (Duperthuy et al., 2011). After extensive washing, the cells were fixed with sterile seawater containing 2.5% glutaraldehyde for 1 h. Post-fixation was achieved in 1% osmium tetraoxide for 1 h at room temperature in the dark. Excess fixing agents were eliminated during dehydration of samples in a graded series of aqueous solution containing increasing amounts of ethanol finishing by absolute acetone. Finally, dehydrated samples were embedded in epoxy resin (EmBed 812). Sections (70 nm thick) were stained with uranyl acetate. All preparations were

examined under a Hitachi 7100 transmission electron microscope at the CRIC platform of Montpellier, France.

Uptake of PKH26-labeled OMVs by oyster hemocytes

OMVs (2 mg ml^{-1}) were labeled with 10^{-6} M PKH26 red fluorescent dye (MINI26-Sigma) as described previously (Duperthuy et al., 2013). After two washes in PBS followed by a 1 h-centrifugation at 100 000 *g*, the PKH26-labeled OMVs were resuspended in PBS. Monolayers of 5×10^5 hemocytes obtained by dispensing freshly collected hemolymph on glass coverslips in a 24-well plate (Costar 3526) were exposed for 2 h to PKH26-labeled OMVs (60 µg per well). After fixation with 4% paraformaldehyde in SSW, hemocytes were washed twice with PBS and stained with 0.5 µg mL^{-1} Phalloidin Alexa488 (Invitrogen) and 0.25 µg mL^{-1} DAPI (Sigma). Photographs were acquired on a Leica SPE confocal laser scanning system connected to a Leica DM2500 upright microscope.

Antimicrobial assays

Serial dilutions of OMVs (6.25 to 50 µg ml^{-1}) were co-incubated with different concentrations of Polymyxin B (PmB, Fluka P9602) for 1 h at 20°C prior to liquid growth inhibition assay using LGP32. Liquid growth inhibition assays were performed in microtiter plates as described in (Hetru and Bulet, 1997) using exponential phase cultures of LGP32 diluted in fresh in Zobell medium at a theorical starting OD_{600} of 0.001. Incubation was performed for 16 h at 20°C and bacterial density was determined spectrophotometrically at 600 nm by using a Multiscan microplate reader (LabSystem). The minimal Inhibitory concentration (MIC) was determined as the lower PmB concentration inhibiting 100% growth.

High-performance liquid chromatography (HPLC) and SDS-PAGE monitoring of PmB

PmB (30 µg) was co-incubated with OMVs (100 µg) or sterile water for 4 h and 6 h at 20°C. Samples (50 µl) were analysed by C18 reversed-phase high performance liquid chromatography (RP-HPLC) column (UP5ODB 25QS, 120 Å, 5 µm, 250 x 2.0 mm, Interchim) using a linear 0-70 % gradient of acetonitrile in 0.05 % TFA over 35 min at a flow rate of 0.7 ml min^{-1}. In parallel, PmB (0.6 µg) was co-incubated with OMVs (2 µg) or sterile water for 4 h at 20°C. Samples were separated on a 12.5 % Tris-Glycine sodium dodecyl sulfate-polyacrylamide gel and stained with silver nitrate.

Acknowledgements

We are grateful to Agnès Vergnes, Julie Nicod and Marc Leroy for technical assistance. We are indebted to Chantal Cazevieille (Centre de Ressources en Imagerie Cellulaire de Montpellier, France) for precious expertise in electron microscopy, as well as to the Montpellier RIO Imaging platform of

University of Montpellier 2 for access to confocal microscopy. We also thank Dr Alain Givaudan, Dr Michel Vidal, Dr Evelyne Bachère, Dr Julien de Lorgeril and Prof. Estelle Jumas-Bilak at the University of Montpellier for fruitful discussions. This work received financial support from the ANR (Vibriogen project, Blanc SVSE7 2011). A.S.V. received fellowship from the Ifremer and the University of Montpellier 1 (graduate student grant).

References

Bagos, P.G., Tsirigos, K.D., Liakopoulos, T.D., and Hamodrakas, S.J. (2008) Prediction of lipoprotein signal peptides in Gram-positive bacteria with a Hidden Markov Model. *J Proteome Res* **7**: 5082-5093.

Balsalobre, C., Silvan, J.M., Berglund, S., Mizunoe, Y., Uhlin, B.E., and Wai, S.N. (2006) Release of the type I secreted alpha-haemolysin via outer membrane vesicles from *Escherichia coli*. *Mol Microbiol* **59**: 99-112.

Bari, W., Lee, K.M., and Yoon, S.S. (2012) Structural and functional importance of outer membrane proteins in *Vibrio cholerae* flagellum. *J Microbiol* **50**: 631-637.

Berven, F.S., Karlsen, O.A., Straume, A.H., Flikka, K., Murrell, J.C., Fjellbirkeland, A. et al. (2006) Analysing the outer membrane subproteome of *Methylococcus capsulatus* (Bath) using proteomics and novel biocomputing tools. *Arch Microbiol* **184**: 362-377.

Beveridge, T.J. (1999) Structures of gram-negative cell walls and their derived membrane vesicles. *J Bacteriol* **181**: 4725-4733.

Binesse, J., Delsert, C., Saulnier, D., Champomier-Verges, M.C., Zagorec, M., Munier-Lehmann, H. et al. (2008) Metalloprotease Vsm is the major determinant of toxicity for extracellular products of *Vibrio splendidus. Appl Environ Microbiol* **74**: 7108-7117.

Boardman, B.K., Meehan, B.M., and Fullner Satchell, K.J. (2007) Growth phase regulation of *Vibrio cholerae* RTX toxin export. *J Bacteriol* **189**: 1827-1835.

Brennan, C.A., Hunt, J.R., Kremer, N., Krasity, B.C., Apicella, M.A., McFall-Ngai, M.J., and Ruby, E.G. (2014) A model symbiosis reveals a role for sheathed-flagellum rotation in the release of immunogenic lipopolysaccharide. *Elife* **3**: e01579.

Chatterjee, D., and Chaudhuri, K. (2011) Association of cholera toxin with *Vibrio cholerae* outer membrane vesicles which are internalized by human intestinal epithelial cells. *FEBS Lett* **585**: 1357-1362.

Chatterjee, S.N., and Das, J. (1967) Electron microscopic observations on the excretion of cell-wall material by *Vibrio cholerae*. *J Gen Microbiol* **49**: 1-11.

Deatherage, B.L., Lara, J.C., Bergsbaken, T., Rassoulian Barrett, S.L., Lara, S., and Cookson, B.T. (2009) Biogenesis of bacterial membrane vesicles. *Mol Microbiol* **72**: 1395-1407.

Defer, D., Desriac, F., Henry, J., Bourgougnon, N., Baudy-Floc'h, M., Brillet, B. et al. (2013) Antimicrobial peptides in oyster hemolymph: the bacterial connection. *Fish Shellfish Immunol* **34**: 1439-1447.

Duperthuy, M., Sjostrom, A.E., Sabharwal, D., Damghani, F., Uhlin, B.E., and Wai, S.N. (2013) Role of the *Vibrio cholerae* Matrix Protein Bap1 in Cross-Resistance to Antimicrobial Peptides. *PLoS Pathog* **9**: e1003620.

Duperthuy, M., Binesse, J., Le Roux, F., Romestand, B., Caro, A., Got, P. et al. (2010) The major outer membrane protein OmpU of *Vibrio splendidus* contributes to host antimicrobial peptide resistance and is required for virulence in the oyster *Crassostrea gigas*. *Environ Microbiol* **12**: 951-963.

Duperthuy, M., Schmitt, P., Garzón, E., Caro, A., Rosa, R.D., Le Roux, F. et al. (2011) Use of OmpU porins for attachment and invasion of *Crassostrea gigas* immune cells by the oyster pathogen *Vibrio splendidus*. *Proc Natl Acad Sci U S A* **108**: 2993-2998.

Dupierris, V., Masselon, C., Court, M., Kieffer-Jaquinod, S., and Bruley, C. (2009) A toolbox for validation of mass spectrometry peptides identification and generation of database: IRMa. *Bioinformatics* **25**: 1980-1981.

Ellis, T.N., and Kuehn, M.J. (2010) Virulence and immunomodulatory roles of bacterial outer membrane vesicles. *Microbiol Mol Biol Rev* **74**: 81-94.

Fernandez-Moreira, E., Helbig, J.H., and Swanson, M.S. (2006) Membrane vesicles shed by *Legionella pneumophila* inhibit fusion of phagosomes with lysosomes. *Infect Immun* **74**: 3285-3295.

Fuerst, J.A., and Perry, J.W. (1988) Demonstration of lipopolysaccharide on sheathed flagella of *Vibrio cholerae* O:1 by protein A-gold immunoelectron microscopy. *J Bacteriol* **170**: 1488-1494.

Gay, M., Renault, T., Pons, A.M., and Le Roux, F. (2004) Two *vibrio splendidus* related strains collaborate to kill *Crassostrea gigas*: taxonomy and host alterations. *Dis Aquat Organ* **62**: 65-74.

Hetru, C., and Bulet, P. (1997) Strategies for the isolation and characterization of antimicrobial peptides of invertebrates. *Methods Mol Biol* **78**: 35-49.

Hiller, K., Grote, A., Scheer, M., Munch, R., and Jahn, D. (2004) PrediSi: prediction of signal peptides and their cleavage positions. *Nucleic Acids Res* **32**: W375-379.

Hong, G.E., Kim, D.G., Park, E.M., Nam, B.H., Kim, Y.O., and Kong, I.S. (2009) Identification of *Vibrio anguillarum* outer membrane vesicles related to immunostimulation in the Japanese flounder, *Paralichthys olivaceus*. *Biosci Biotechnol Biochem* **73**: 437-439.

Imai, K., Asakawa, N., Tsuji, T., Akazawa, F., Ino, A., Sonoyama, M., and Mitaku, S. (2008) SOSUI-GramN: high performance prediction for sub-cellular localization of proteins in gram-negative bacteria. *Bioinformation* **2**: 417-421.

Kall, L., Krogh, A., and Sonnhammer, E.L. (2004) A combined transmembrane topology and signal peptide prediction method. *J Mol Biol* **338**: 1027-1036.

Kaplan, E.L., and Meier, P. (1958) Non parametric estimation for incomplete observations. *J Am Stat Assoc* **53**: 457-481.

Kim, Y.R., Kim, B.U., Kim, S.Y., Kim, C.M., Na, H.S., Koh, J.T. et al. (2010) Outer membrane vesicles of *Vibrio vulnificus* deliver cytolysin-hemolysin VvhA into epithelial cells to induce cytotoxicity. *Biochem Biophys Res Commun* **399**: 607-612.

Kobayashi, H., Utsunomiya, H., Yamanaka, H., Sei, Y., Katunuma, N., Okamoto, K., and Tsuge, H. (2009) Structural basis for the kexin-like serine protease from Aeromonas sobria as sepsis-causing factor. *J Biol Chem* **284**: 27655-27663.

Kremer, N., Philipp, E.E., Carpentier, M.C., Brennan, C.A., Kraemer, L., Altura, M.A. et al. (2013) Initial symbiont contact orchestrates host-organ-wide transcriptional changes that prime tissue colonization. *Cell Host Microbe* **14**: 183-194.

Krogh, A., Larsson, B., von Heijne, G., and Sonnhammer, E.L. (2001) Predicting transmembrane protein topology with a hidden Markov model: application to complete genomes. *J Mol Biol* **305**: 567-580.

Kuehn, M.J., and Kesty, N.C. (2005) Bacterial outer membrane vesicles and the host-pathogen interaction. *Genes Dev* **19**: 2645-2655.

Kulp, A., and Kuehn, M.J. (2010) Biological functions and biogenesis of secreted bacterial outer membrane vesicles. *Annu Rev Microbiol* **64**: 163-184.

Labreuche, Y., Soudant, P., Goncalves, M., Lambert, C., and Nicolas, J.L. (2006) Effects of extracellular products from the pathogenic *Vibrio aestuarianus* strain 01/32 on lethality and cellular immune responses of the oyster *Crassostrea gigas*. *Dev Comp Immunol* **30**: 367-379.

Labreuche, Y., Le Roux, F., Henry, J., Zatylny, C., Huvet, A., Lambert, C. et al. (2010) *Vibrio aestuarianus* zinc metalloprotease causes lethality in the Pacific oyster *Crassostrea gigas* and impairs the host cellular immune defenses. *Fish Shellfish Immunol* **29**: 753-758.

Le Roux, F., Binesse, J., Saulnier, D., and Mazel, D. (2007) Construction of a *Vibrio splendidus* mutant lacking the metalloprotease gene *vsm* by use of a novel counterselectable suicide vector. *Appl Environ Microbiol* **73**: 777-784.

Le Roux, F., Zouine, M., Chakroun, N., Binesse, J., Saulnier, D., Bouchier, C. et al. (2009) Genome sequence of *Vibrio splendidus*: an abundant planctonic marine species with a large genotypic diversity. *Environ Microbiol* **11**: 1959-1970.

Lee, E.Y., Choi, D.S., Kim, K.P., and Gho, Y.S. (2008) Proteomics in gram-negative bacterial outer membrane vesicles. *Mass Spectrom Rev* **27**: 535-555.

Lee, H.J., Kim, J.A., Lee, M.A., Park, S.J., and Lee, K.H. (2013) Regulation of haemolysin (VvhA) production by ferric uptake regulator (Fur) in *Vibrio vulnificus*: repression of *vvhA* transcription by Fur and proteolysis of VvhA by Fur-repressive exoproteases. *Mol Microbiol* **88**: 813-826.

Lindell, K., Fahlgren, A., Hjerde, E., Willassen, N.P., Fallman, M., and Milton, D.L. (2012) Lipopolysaccharide O-antigen prevents phagocytosis of Vibrio anguillarum by rainbow trout (Oncorhynchus mykiss) skin epithelial cells. *PLoS One* **7**: e37678.

Liu, P.V. (1957) Survey of hemolysin production among species of pseudomonads. *J Bacteriol* **74**: 718-727.

Manabe, T., Kato, M., Ueno, T., and Kawasaki, K. (2013) Flagella proteins contribute to the production of outer membrane vesicles from *Escherichia coli* W3110. *Biochem Biophys Res Commun* **441**: 151-156.

Manning, A.J., and Kuehn, M.J. (2011) Contribution of bacterial outer membrane vesicles to innate bacterial defense. *BMC Microbiol* **11**: 258.

Manning, A.J., and Kuehn, M.J. (2013) Functional advantages conferred by extracellular prokaryotic membrane vesicles. *J Mol Microbiol Biotechnol* **23**: 131-141.

McKean, S.C., Davies, J.K., and Moore, R.J. (2007) Expression of phospholipase D, the major virulence factor of *Corynebacterium pseudotuberculosis*, is regulated by multiple environmental factors and plays a role in macrophage death. *Microbiology* **153**: 2203-2211.

Méndez, J., Reimundo, P., Pérez-Pascual, D., Navais, R., Gómez, E., Cascales, D., and Guijarro, J.A. (2012) An Overview of Virulence-Associated Factors of Gram-Negative Fish Pathogenic Bacteria. In *Health and Environment in Aquaculture*. Carvalho, D.E. (ed). Rijeka, Croatia: InTech, pp. 133-156.

Miyoshi, S., and Shinoda, S. (2000) Microbial metalloproteases and pathogenesis. *Microbes Infect* **2**: 91-98.

Nizet, V. (2006) Antimicrobial peptide resistance mechanisms of human bacterial pathogens. *Curr Issues Mol Biol* **8**: 11-26.

Olivot, J.M., Labreuche, J., Mahagne, M.H., Aiach, M., and Amarenco, P. (2006) Endogenous tissue-type plasminogen activator and cardioembolic brain infarct subtype. *J Thromb Haemost* **4**: 2513-2514.

Petersen, T.N., Brunak, S., von Heijne, G., and Nielsen, H. (2011) SignalP 4.0: discriminating signal peptides from transmembrane regions. *Nat Methods* **8**: 785-786.

Punta, M., Coggill, P.C., Eberhardt, R.Y., Mistry, J., Tate, J., Boursnell, C. et al. (2012) The Pfam protein families database. *Nucleic Acids Res* **40**: D290-301.

Quevillon, E., Silventoinen, V., Pillai, S., Harte, N., Mulder, N., Apweiler, R., and Lopez, R. (2005) InterProScan: protein domains identifier. *Nucleic Acids Res* **33**: W116-120.

Rahman, O., Cummings, S.P., Harrington, D.J., and Sutcliffe, I.C. (2008) Methods for the bioinformatic identification of bacterial lipoproteins encoded in the genomes of Gram-positive bacteria. *World Journal of Microbiology and Biotechnology* **24**: 2377-2382.

Rawlings, N.D., Barrett, A.J., and Bateman, A. (2012) MEROPS: the database of proteolytic enzymes, their substrates and inhibitors. *Nucleic Acids Res* **40**: D343-350.

Remmert, M., Linke, D., Lupas, A.N., and Soding, J. (2009) HHomp--prediction and classification of outer membrane proteins. *Nucleic Acids Res* **37**: W446-451.

Rompikuntal, P.K., Thay, B., Khan, M.K., Alanko, J., Penttinen, A.M., Asikainen, S. et al. (2012) Perinuclear localization of internalized outer membrane vesicles carrying active cytolethal distending toxin from *Aggregatibacter actinomycetemcomitans*. *Infect Immun* **80**: 31-42.

Rose, R.W., Bruser, T., Kissinger, J.C., and Pohlschroder, M. (2002) Adaptation of protein secretion to extremely high-salt conditions by extensive use of the twin-arginine translocation pathway. *Mol Microbiol* **45**: 943-950.

Sawabe, T., Ogura, Y., Matsumura, Y., Feng, G., Amin, A.R., Mino, S. et al. (2013) Updating the Vibrio clades defined by multilocus sequence phylogeny: proposal of eight new clades, and the description of *Vibrio tritonius* sp. nov. *Front Microbiol* **4**: 414.

Schmitt, P., Duperthuy, M., Montagnani, C., Bachère, E., and Destoumieux-Garzón, D. (2011) Immune responses in the Pacific oyster *Crassostrea gigas*. An overview with focus on summer mortalities. In *Oysters: physiology, ecological distribution and mortality*. Qin, J. (ed): Nova Science Publishers, Inc. pp227-273

Schmitt, P., Rosa, R.D., Duperthuy, M., de Lorgeril, J., Bachere, E., and Destoumieux-Garzon, D. (2012) The Antimicrobial Defense of the Pacific Oyster, *Crassostrea gigas*. How Diversity may Compensate for Scarcity in the Regulation of Resident/Pathogenic Microflora. *Front Microbiol* **3**: 160.

Shinoda, S., and Miyoshi, S. (2011) Proteases produced by vibrios. *Biocontrol Sci* **16**: 1-11.

Sikora, A.E., Zielke, R.A., Lawrence, D.A., Andrews, P.C., and Sandkvist, M. (2011) Proteomic analysis of the *Vibrio cholerae* type II secretome reveals new proteins, including three related serine proteases. *J Biol Chem* **286**: 16555-16566.

Tomarelli, R.M., Charney, J., and Harding, M.L. (1949) The use of azoalbumin as a substrate in the colorimetric determination or peptic and tryptic activity. *J Lab Clin Med* **34**: 428-433.

Tusnady, G.E., and Simon, I. (2001) The HMMTOP transmembrane topology prediction server. *Bioinformatics* **17**: 849-850.

Vallenet, D., Belda, E., Calteau, A., Cruveiller, S., Engelen, S., Lajus, A. et al. (2013) MicroScope--an integrated microbial resource for the curation and comparative analysis of genomic and metabolic data. *Nucleic Acids Res* **41**: D636-647.

Wai, S.N., Takade, A., and Amako, K. (1995) The release of outer membrane vesicles from the strains of enterotoxigenic *Escherichia coli*. *Microbiol Immunol* **39**: 451-456.

Wai, S.N., Lindmark, B., Soderblom, T., Takade, A., Westermark, M., Oscarsson, J. et al. (2003) Vesicle-mediated export and assembly of pore-forming oligomers of the enterobacterial ClyA cytotoxin. *Cell* **115**: 25-35.

Yozwiak, M.L., and Songer, J.G. (1993) Effect of *Corynebacterium pseudotuberculosis* phospholipase D on viability and chemotactic responses of ovine neutrophils. *Am J Vet Res* **54**: 392-397.

Yu, C.S., Chen, Y.C., Lu, C.H., and Hwang, J.K. (2006) Prediction of protein subcellular localization. *Proteins* **64**: 643-651.

Yu, N.Y., Wagner, J.R., Laird, M.R., Melli, G., Rey, S., Lo, R. et al. (2010) PSORTb 3.0: improved protein subcellular localization prediction with refined localization subcategories and predictive capabilities for all prokaryotes. *Bioinformatics* **26**: 1608-1615.

Zhang, X.H., and Austin, B. (2005) Haemolysins in *Vibrio* species. *J Appl Microbiol* **98**: 1011-1019.

Table 1. Minimum inhibitory concentration (MIC) of Polymyxin B in the presence/absence of OMVs from wild-type and *Δvsp* LGP32.

strain	OMVs (μg ml^{-1})		MIC of PmB (μM)
	wild-type	*Δvsp*	
wild-type LGP32	0	0	0.78
wild-type LGP32	6.25	0	1.56
wild-type LGP32	12.5	0	3.12
wild-type LGP32	25	0	6.25
wild-type LGP32	50	0	12.5
wild-type LGP32	0	50	12.5
Δvsp LGP32	0	0	0.78

Legends

Fig. 1. *Vibrio tasmaniensis* LGP32 secretes outer membrane vesicles

A-E. Transmission electron microscopy of negatively-stained LGP32 cultures in logarithmic phase of growth. Extracellular vesicles produced by LGP32 (black arrows) are observed detaching from outer membrane (A-B) or from the polar flagellum (C-E). B. Enlarged part of the picture A.

F. Transmission electron microscopy of negatively-stained vesicles obtained by ultracentrifugation. The vesicle diameters range from 30 to 50 nm.

Fig. 2. Proteases are encapsulated in LGP32 OMVs.

A. Protease activity was determined by azocasein hydrolysis (absorbance 440 nm) on 1 mg ml^{-1} ultracentrifuged supernatant of LGP32 ECPs (Sn) as well as on 2 mg ml^{-1} OMVs from LGP32 lysed in 0.1% triton X-100 or resuspended in PBS (intact OMVs). Data were generated from three independent ECPs preparations. Data are the mean of three independent OMVs production +/- SEM.

B. Zymography showing gelatin hydrolysis (clear zone) by OMVs preparations from wild-type and Δ*vsp* LGP32 vibrios. Molecular masses are indicated on the right.

C. Transmission electron microscopy of negatively-stained vesicles resuspended in PBS (intact) or lysed in 0.1% triton X-100.

Fig. 3. The intravesicular Vsp protease is a homologue of the serine protease VesA

Peptides identified by MS-MS sequencing after trypsin digestion of the zymography active band (boxes) are displayed on the amino acid sequence deduced from the VS_II0815 (Vsp) nucleic acid sequence. The sequences of LGP32 Vsp and *Vibrio cholera* VesA (VCA0803) were aligned with ClustalW. Identical amino acids are indicated by an asterisk. Conservative replacements are indicated by a colon. Conserved amino acids involved in the catalytic triad of serine proteases (His95, Asp149, Ser254) are highlighted in black. Conserved positions of predicted cysteine bridges are indicated with hooks. The predicted signal peptides are underlined. The transmembrane helices predicted with Phobius and TMHMM are highlighted in grey. Amino acids are numbered on the right.

Fig. 4. The virulence of the Δ*vsp* mutant is attenuated in oyster experimental infections

Kaplan-Meier survival curves from oyster infection experiments. Juvenile oyster were injected with 4 x 10^7 cfu per animal of the wild-type LGP32 (square) or the isogenic *Δvsp* (triangle) mutant. An injection of sterile seawater (SSW) was used as control (circle). Groups of 45 oysters (15 per seawater

tank) were monitored for 7 days after infection. Data are representative of two independent experiments.

Fig. 5. Intracellular and extracellular delivery of OMVs to oyster immune cells

A and C. MET observation of oyster hemocytes containing intraphagosomal LGP32 after phagocytosis (30 min-contact).

A. Two intracellular LGP32 are observed together with one extracellular LGP32. The hemocyte does not show any evidence of cell damage.

B. Enlarged part of the picture in A showing the release of OMVs by intraphagosomal LGP32 (black arrows).

C-D. Oyster hemocytes containing numerous intracellular LGP32 display major alterations including loss of organelle integrity and damages to the cytoplasmic and the phagosomal membranes (white arrows).

E. Confocal microscopy section showing the internalization of PKH26-labeled OMVs (red) by most hemocytes after 2h of incubation *in vitro* (white arrows). Hemocyte nuclei were stained with DAPI (blue). F-actin was stained with phalloidin (green).

F. Enlarged part of the picture in C showing the intracellular localization of PKH26-labeled OMVs.

Fig. 6. Polymyxin B is titrated but not degraded by *V. splendidus* LGP32 OMVs.

A. Silver-stained Tris-tricine SDS-PAGE of PmB (0.6 µg) incubated for 6 h in the presence (+) / absence (-) of 2 µg OMVs. Molecular masses (kDa) are shown on the right.

B. Time-course of PmB titration by wild-type OMVs monitored by RP-HPLC. PmB (30 µg) was incubated with 100 µg OMVs. The PmB trace (arrow) was monitored at 0, 4 and 6h on a UP5-ODB-25QS column using a 0-70% acetonitrile gradient over 35 min.

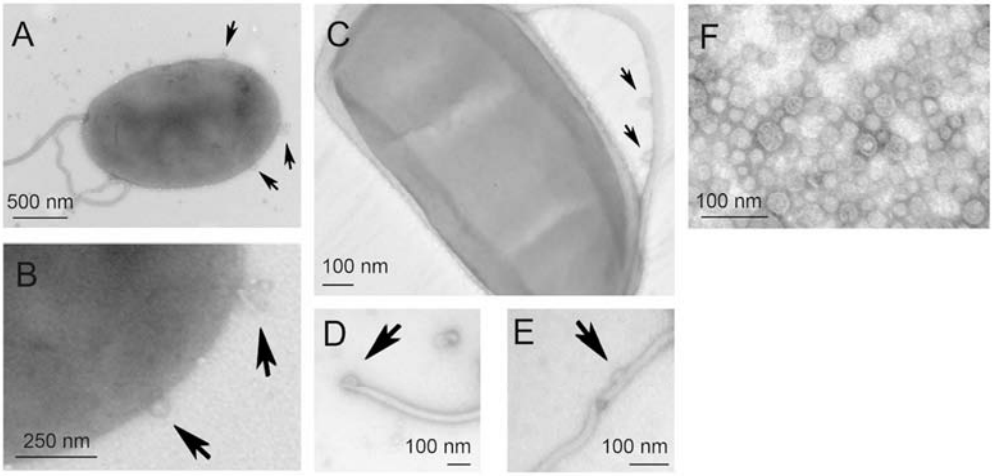

Fig. 1. Vibrio tasmaniensis LGP32 secretes outer membrane vesicles
A-E. Transmission electron microscopy of negatively-stained LGP32 cultures in logarithmic phase of growth. Extracellular vesicles produced by LGP32 (black arrows) are observed detaching from outer membrane (A-B) or from the polar flagellum (C-E). B. Enlarged part of the picture A.
F. Transmission electron microscopy of negatively-stained vesicles obtained by ultracentrifugation. The vesicle diameters range from 30 to 50 nm.

109x53mm (300 x 300 DPI)

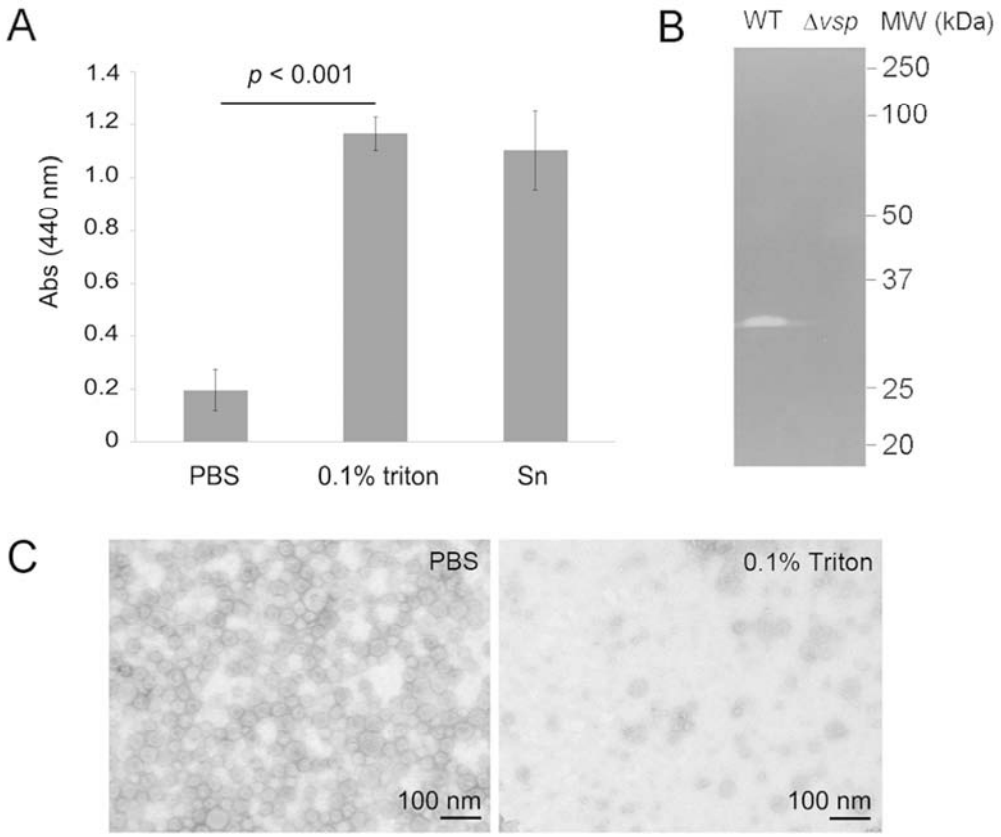

Fig. 2. Proteases are encapsulated in LGP32 OMVs.
A. Protease activity was determined by azocasein hydrolysis (absorbance 440 nm) on 1 mg ml-1 ultracentrifuged supernatant of LGP32 ECPs (Sn) as well as on 2 mg ml-1 OMVs from LGP32 lysed in 0.1% triton X-100 or resuspended in PBS (intact OMVs). Data were generated from three independent ECPs preparations. Data are the mean of three independent OMVs production +/- SEM.
B. Zymography showing gelatin hydrolysis (clear zone) by OMVs preparations from wild-type and Δvsp LGP32 vibrios. Molecular masses are indicated on the right.
C. Transmission electron microscopy of negatively-stained vesicles resuspended in PBS (intact) or lysed in 0.1% triton X-100.

80x66mm (300 x 300 DPI)

```
Vsp    MNVNHTMSPVRKAVLGLLAPLIYTSSVMATENSVESAPNVGVSPYIVNGS  50
VesA           MRK---WLWLLLLLTTRVSAVE---------ISPYIVNGT  28
               :**    *   *: *: * * *          :*******:

Vsp    NASVTDFPSMASLFIDRIDYDGVYSTGSYCGATILDPSHVLTAAHCIYGD 100
VesA   NANVANYPSFASLAIYISPYQ--YSSGTYCGATVLNSRYILTAAHCIYGN  76
       ** *:::**:*** *    *:  **:*:*****:*:  ::*********:

Vsp    EEGQLFTVVVPQIEDTSQFPKGNIQKARVSEVYYPSDYSDEISDFLRNDV 150
VesA   SYTMLYTVVVPQLEDESQFPNGNVQLARAAEFYYPDNYVDSSAVYWPNDI 126
           *:******:** ****:**:* ** :* *** :* *  : :  **:

Vsp    AILKLESALNVDSINDVVKRPSNETYRNAASDFVAVGHGNTRTGFDGTTL 200
VesA   AIIKLESDLNVSNFVGVLNSSINNSY-DENGTYKAIGHGYVNGNVAGGTR 175
       **:**** ***..: .*:: . *::* :  . : *:*** .. .. * *

Vsp    LQKVTLAYVDNTTCKNAFTGKDNPNPPLTGKQICFTGDFNIFTSLYGSTC 250
VesA   LLETTLTFVPFATCS-AYYGAN-----LGPGHVCFTG--PQIGSYRNSTC 217
       * : **::*  :**  *: * :     *   ::****    : *   ***

Vsp    QGDSGGPVYWKDGSDYRQVGITSFGPATCGGNSV-VTSVFTEIYDYRDWI 299
VesA   SGDSGGPVYWDSGSGYVQIGITSFGPSTCGNPALPVTSVFTEVSDYYSWI 267
        *********  ** * *:*******:***  :: *******: **  **

Vsp    DSVIAGTETAKFVSTHAK--RSAYSGLKKKPVTSSGSSGGSVSFSLLGML 347
VesA   LRVMNGLETPKYYVTESNGVRQLVAGGTTTVSVSESSSGGGVSLLIAFFL 317
         *: * ** *:  * ::  *   :*       *  **** **: :  :*

Vsp    MLFAGFRTFNRFRK 361
VesA   GMLMIIRRNN-LKI 330
         ::  :*  * ::
```

Fig. 3. The intravesicular Vsp protease is a homologue of the serine protease VesA
Peptides identified by MS-MS sequencing after trypsin digestion of the zymography active band (boxes) are displayed on the amino acid sequence deduced from the VS_II0815 (Vsp) nucleic acid sequence. The sequences of LGP32 Vsp and Vibrio cholera VesA (VCA0803) were aligned with ClustalW. Identical amino acids are indicated by an asterisk. Conservative replacements are indicated by a colon. Conserved amino acids involved in the catalytic triad of serine proteases (His95, Asp149, Ser254) are highlighted in black. Conserved positions of predicted cysteine bridges are indicated with hooks. The predicted signal peptides are underlined. The transmembrane helices predicted with Phobius and TMHMM are highlighted in grey. Amino acids are numbered on the right.

80x114mm (300 x 300 DPI)

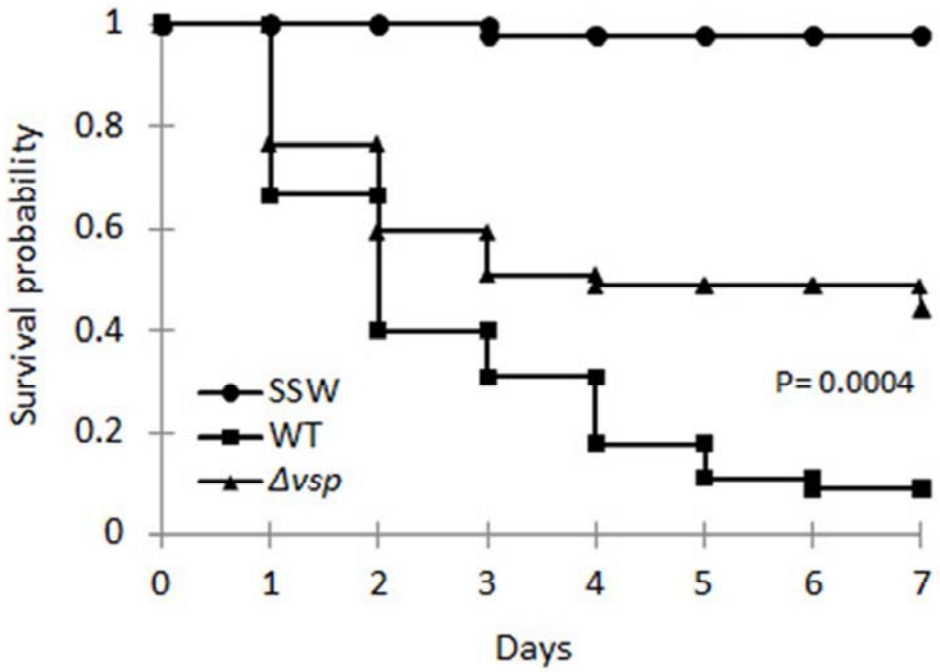

Fig. 4. The virulence of the ∆vsp mutant is attenuated in oyster experimental infections
Kaplan-Meier survival curves from oyster infection experiments. Juvenile oyster were injected with 4 x 107 cfu per animal of the wild-type LGP32 (square) or the isogenic Δvsp (triangle) mutant. An injection of sterile seawater (SSW) was used as control (circle). Groups of 45 oysters (15 per seawater tank) were monitored for 7 days after infection. Data are representative of two independent experiments.

79x58mm (150 x 150 DPI)

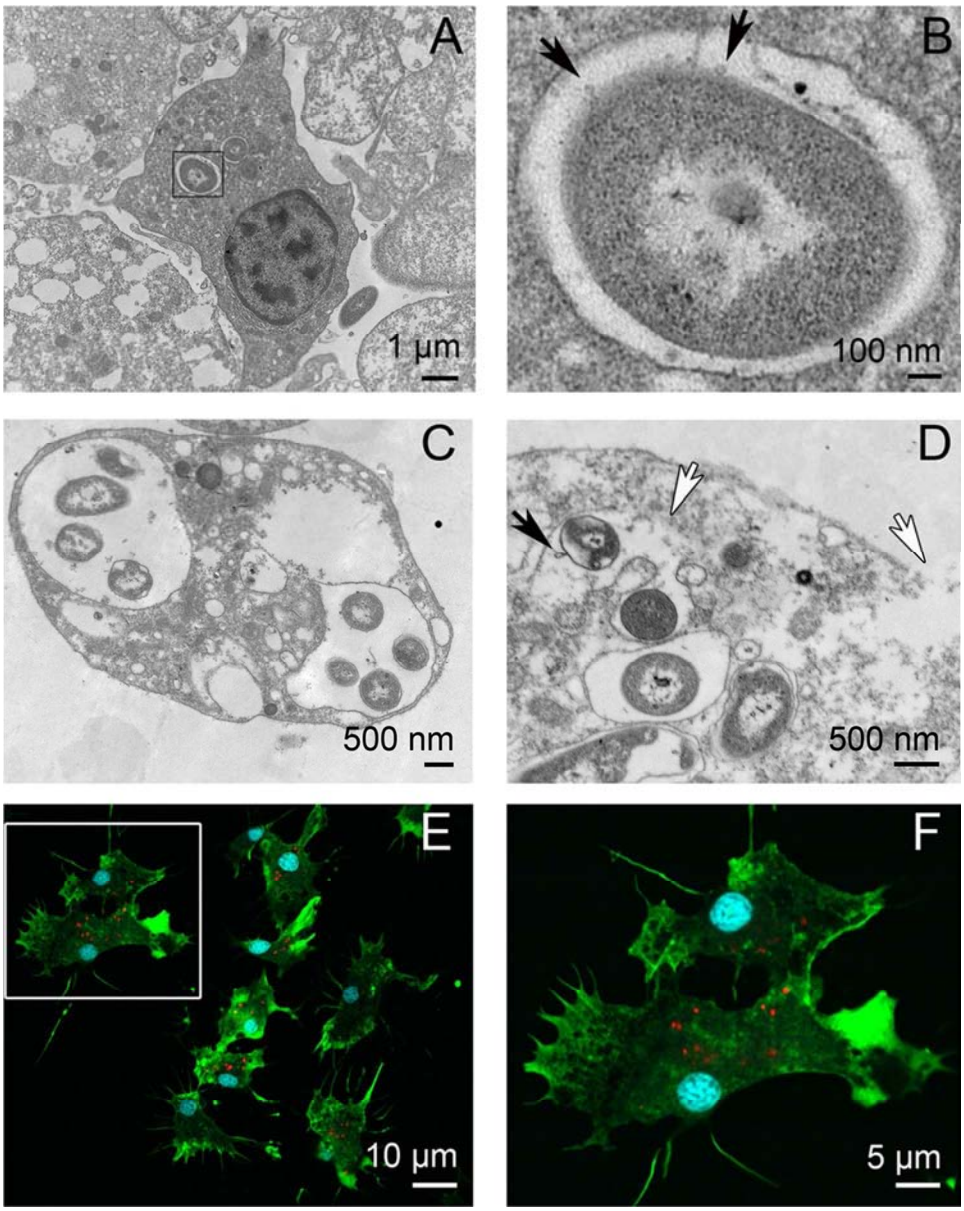

Fig. 5. Intracellular and extracellular delivery of OMVs to oyster immune cells
A and C. MET observation of oyster hemocytes containing intraphagosomal LGP32 after phagocytosis (30 min-contact).
A. Two intracellular LGP32 are observed together with one extracellular LGP32. The hemocyte does not show any evidence of cell damage.
B. Enlarged part of the picture in A showing the release of OMVs by intraphagosomal LGP32 (black arrows).
C-D. Oyster hemocytes containing numerous intracellular LGP32 display major alterations including loss of organelle integrity and damages to the cytoplasmic and the phagosomal membranes (white arrows).
E. Confocal microscopy section showing the internalization of PKH26-labeled OMVs (red) by most hemocytes after 2h of incubation in vitro (white arrows). Hemocyte nuclei were stained with DAPI (blue). F-actin was stained with phalloidin (green).
F. Enlarged part of the picture in C showing the intracellular localization of PKH26-labeled OMVs.

80x100mm (300 x 300 DPI)

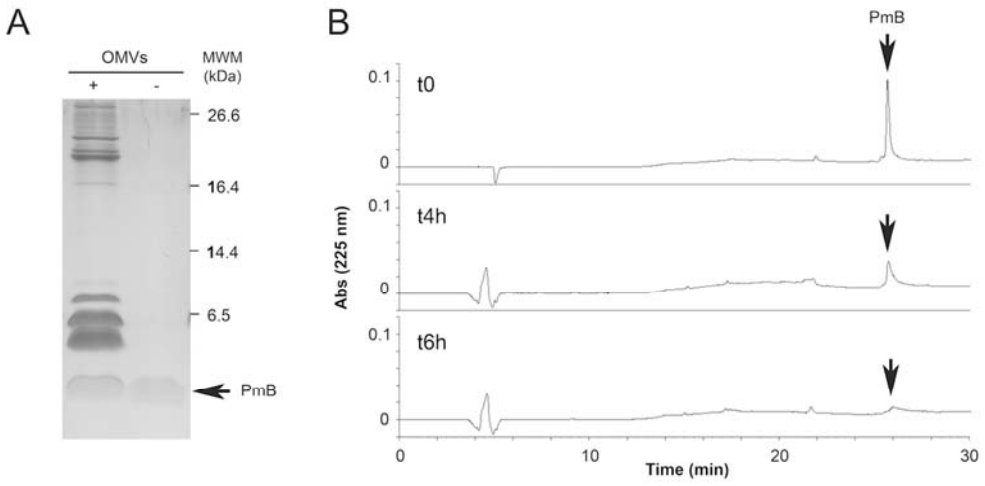

Fig. 6. Polymyxin B is titrated but not degraded by V. splendidus LGP32 OMVs.
A. Silver-stained Tris-tricine SDS-PAGE of PmB (0.6 µg) incubated for 6 h in the presence (+) / absence (-) of 2 µg OMVs. Molecular masses (kDa) are shown on the right.
B. Time-course of PmB titration by wild-type OMVs monitored by RP-HPLC. PmB (30 µg) was incubated with 100 µg OMVs. The PmB trace (arrow) was monitored at 0, 4 and 6h on a UP5-ODB-25QS column using a 0-70% acetonitrile gradient over 35 min.

109x53mm (300 x 300 DPI)

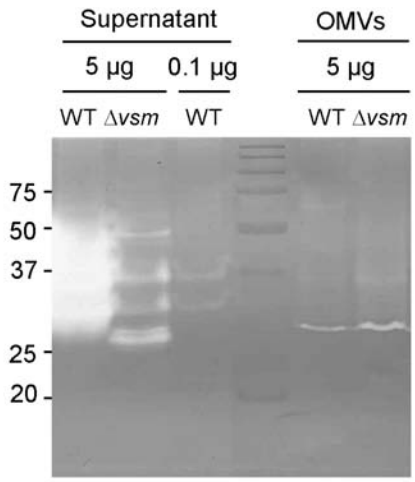

Figure S1. The major protease of OMVs is not the major extracellular metalloprotease Vsm.

Characterization of the protease activity associated to OMVs. Zymography showing gelatin hydrolysis by OMVs (pellets, 5 µg) or ultracentrifuge supernatants (5 or 0.1 µg) from the wild-type and Δ*vsm*LGP32. Molecular masses (kDa) are shown on the left. The active band of wild-type OMVs is maintained in the Δ*vsm* mutant. No band at the same molecular mass is visible in ultracentrifuge supernatants of the WT and Δ*vsm* mutant.

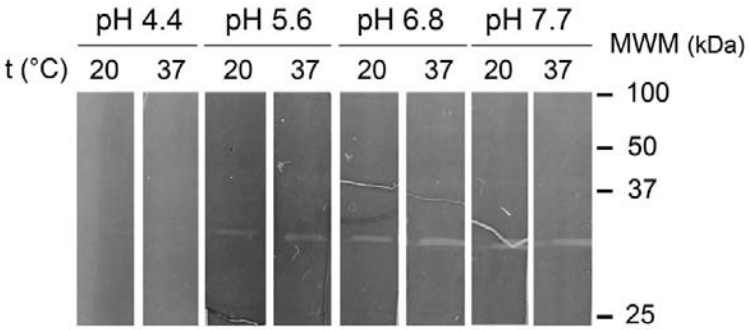

Figure S2. Vsp activity is stable in a pH range of 5.6 to 7.7.

Zymography showing gelatin hydrolysis by OMVs from the wild-type LGP32 (10µg) at 20°C and 37°C in 50 mM citrate buffer pH 4.4 or 50mM phosphate buffer pH 5.6, 6.8 and 7.7. Molecular masses are shown on the right.

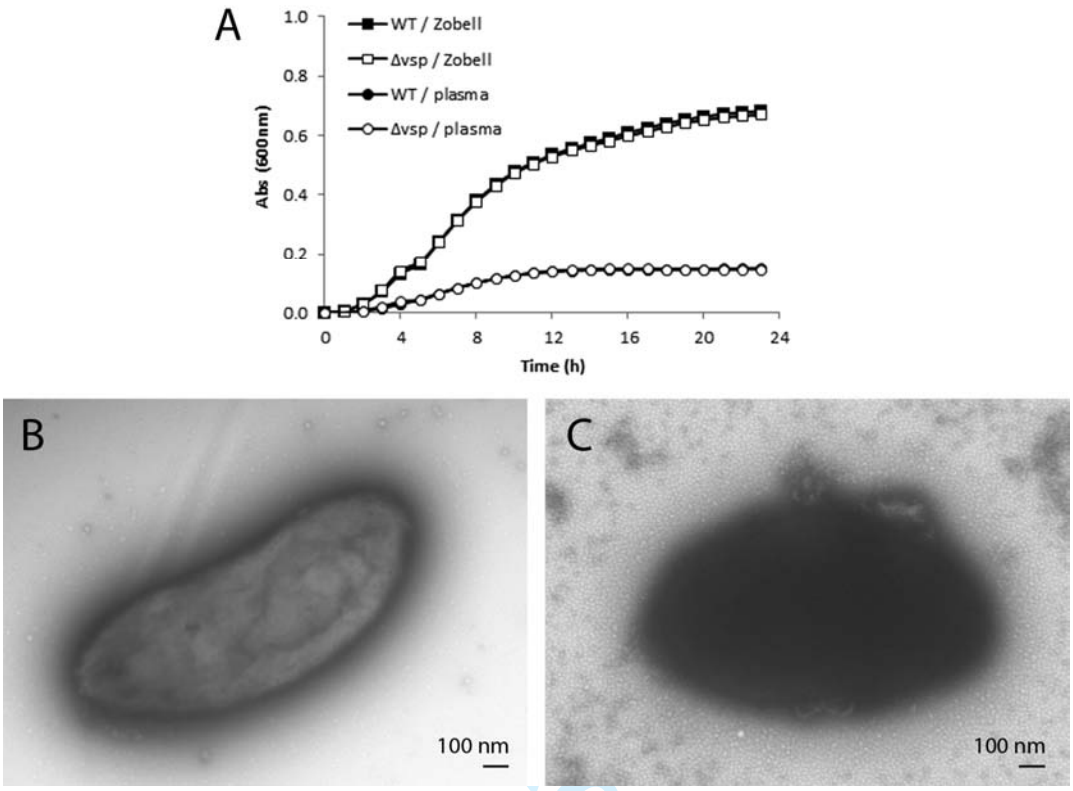

Figure S3. Effect of plasma on LGP32 growth and OMV production.

(A) Growth curves of wild-type (WT) LGP32 (black) and its isogenic *Δvsp* mutant (white) were obtained in Zobell medium (squares) and oyster plasma (circles) at a temperature of 20°C. Culture turbidity was monitored at 600 nm every 1h.The *vsp* deletion did not impair growth of LGP32 in Zobell medium nor in plasma. (B-C) Transmission electron microscopy of negatively-stained wild-type LGP32 cultures in Zobell medium (B) and filtered oyster plasma (C). While only few OMVs were released in Zobell medium (A), a massive release of OMVs was observed in plasma (B).

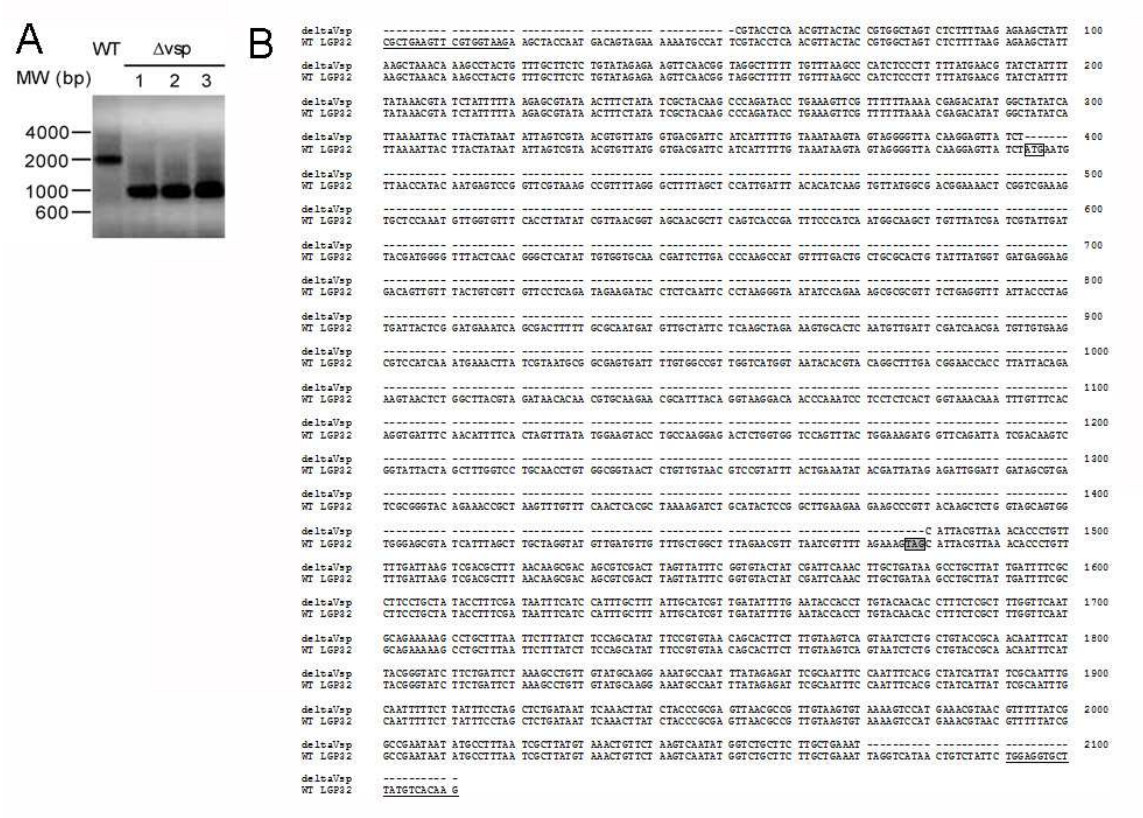

Figure S4. Control of *vsp* gene deletion.

A. PCR amplification of the DNA region flanking the *vsp* gene. DNA extracted from the wild-type (WT) and the three Δ*vsp* mutants (1,2,3) was amplified using the VS_II0815-Fw2 and VS_II0815-Rv2 external primers (Table S3). The molecular weight marker is displayed on the left. The expected size for the wild-type and Δ*vsp* amplicon are 2111 bp and 1025 bp, respectively.

B. Control of *vsp* deletion by sequencing. The PCR-amplified fragments obtained from the Δ*vsp*1, 2 and 3 mutants were sequenced. Sequences were aligned with that of wild-type LGP32 using ClustalW. Gaps corresponding to the deletion are indicated by dashes. The VS_II0815-Fw2 and VS_II0815-Rv2 primers used for sequencing are underlined. The ATG and stop codons of the *vsp* open-reading frame are displayed in white and grey boxes, respectively.

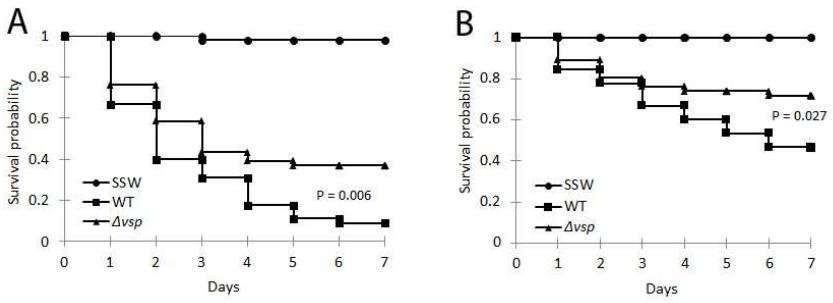

Figure S5. Attenuated virulence of two additional Δ*vsp* mutants is in oyster experimental infections. Kaplan-Meier survival curves were generated from 45 juvenile (A) or adult (B) oysters injected with wild-type (square) or Δ*vsp* (triangle) LGP32 (4 x 10^7 CFU per juvenile oyster or 2 x 10^8 CFU per adult oyster). An injection of sterile seawater (SSW) was used as control (circle). Two Δ*vsp* mutants obtained independently were used in experimental infections (A) and (B). Oysters (15 per seawater tank) were monitored for 7 days after infection.

Table S1. List of proteins associated to *V. splendidus* LGP32 OMVs.

Protein identification was carried out by comparing experimentally generated monoisotopic peaks of peptides with computer-generated fingerprints using the Mascot program. Mascot was run on protein sequences deduced from four sequenced *V. splendidus* LGP32 genome (Le Roux et al., 2009). Only proteins identified by more than 3 peptides in two independent OMV preparations are displayed. OMV prep #1 was crude while OMV prep #2 was purified by density gradient. Only proteins found in both preparations are displayed. P, M, N, and L stand for protease, murein hydrolase, nuclease, and lipase, respectively. OM and IM stand for outer and inner membrane, respectively. The Vsp line is displayed in boldface.

						OMV prep #1 (crude)		OMV prep #2 (purified on density gradient)	
Accession	**Gene**	**Function**	**Localisation**	**Signal Peptide**	**Activity**	**Coverage**	**Peptides**	**Coverage**	**Peptides**
Enzyme activity									
VS_0358	*mdh*	Malate dehydrogenase	Sec exported	yes		16.0	3	40.1	7
VS_0372	*surA*	Parvulin-like peptidyl-prolyl isomerase, SurA	Sec exported	yes		37.5	13	29.1	8
VS_0426	*degQ*	Protease degQ	Periplasmic	yes	P	31.4	9	13.1	4
VS_0436		Hemolysin	OM (lipo)	yes		24.9	4	19.9	3
VS_0757	*ushA*	5'-nucleotidase	OM (lipo)	yes	N	59.0	30	63.9	31
VS_0885	*mtlB*	Putative membrane-bound lytic murein transglycosylase B	Sec exported	yes	M	12.6	3	24.0	5
VS_0937	*sppA*	Protease IV (Endopeptidase IV)	IM		P	8.3	4	12.1	6
VS_1051		Putative exonuclease	OM	yes	N	31.9	8	9.6	4
VS_1058		Putative peptidase M60-like family protein	OM (lipo)	yes	P	3.1	3	3.5	3
VS_1100		Putative ATP-dependent Zn protease	Sec exported	yes	P	30.0	6	26.3	4
VS_1267	*vsm*	Extracellular zinc metalloprotease (M4 family)	Extracellular	yes	P	37.4	19	31.6	14
VS_1417	*prc*	Carboxy-terminal protease (S41 family)	Sec exported	yes	P	32.5	16	12.8	6
VS_1921		Putative Iron-regulated protein with peptidase M75 domain	OM (lipo)	yes	P	16.2	4	16.2	4
VS_2380	*mliC*	Putative C-type lysozyme inhibitor (MliC)	OM (lipo)	yes		45.6	3	51.8	4
VS_2523		Serine protease	OM	yes	P	17.5	10	13.1	6
VS_2563		Putative lysozyme-like protein	Unknown		M	34.2	6	22.4	3
VS_2565		Putative M16 family zinc peptidase (M16 family)	OM (lipo)	yes	P	24.6	18	10.5	7
VS_2790	*CpdB*	Bifunctional 2',3'-cyclic nucleotide 2'-phosphodiesterase/3'-nucleotidase	OM (lipo)	yes	N	62.4	28	44.2	17
VS_3081	*ggt*	Gamma-glutamyltranspeptidase	Periplasmic	yes		23.7	11	20.8	9
VS_3140	*dsbA*	Thiol:disulfide interchange protein, DsbA	Periplasmic	yes		34.0	7	24.3	4
VS_II0262		Putative pyruvate/2-oxoglutarate dehydrogenase complex, dihydrolipoamide dehydrogenase component	OM (lipo)	yes		38.3	3	50.8	4
VS_II0416		Hemolysin	OM (lipo)	yes		52.3	4	52.3	4
VS_II0492	*pepDB*	Putative dipeptidase B	Sec exported	yes	P	9.2	3	10.7	3
VS_II0598	*napA*	Periplasmic nitrate reductase	Periplasmic	yes		14.9	10	4.5	3
VS_II0716		Putative ATP-dependent Zn	OM (lipo)	yes	P	57.4	12	39.1	8

		protease							
VS_II0771	*oma1*	Zn-dependent peptidase (M48 family)	OM (lipo)	yes	P	35.9	6	17.9	3
VS_II0774		Putative extracellular triacylglycerol lipase	OM (lipo)	yes	L	41.5	20	41.9	21
VS_II0815	***vsp***	**SI family secreted trypsin-like serine protease**	**IM**	**yes**	**P**	**16.0**	**4**	**16.0**	**4**
VS_II0870		Putative alkaline phosphatase	Sec exported	yes		25.0	9	18.1	7
VS_II0879	*aslA*	Putative arylsulfatase A	Periplasmic	yes		45.5	21	42.9	19
VS_II1298	*nepU*	Putativelycosidase	OM (lipo)	yes		26.9	13	4.9	3
VS_II1485		Putative zinc protease (M16 family)	OM (lipo)	yes	P	21.6	15	14.1	11
VS_II1486		Putative zinc protease	OM (lipo)	yes	P	4.6	3	10.1	6
Tranport/Conjugation									
VS_0075	*dppA*	Putative dipeptide ABC transporter, periplasmic binding protein / Cytochrome C	Periplasmic	yes		60.3	25	63.5	23
VS_0213	*wza*	Capsular polysaccharide export protein, Wza	OM (lipo)	yes		26.8	7	29.4	7
VS_0297		Putative ABC-type Fe3+-hydroxamate transport system component	OM	yes		18.7	4	13.1	3
VS_0355		Putative TRAP transporter solute receptor (TAXI family)	Sec exported	yes		65.9	14	67.1	14
VS_0373	*lptD*	Outer membrane lipid A transporter lptD	OM	yes		35.5	22	33.4	21
VS_0418	*tolC*	Outer membrane channel protein, TolC	OM	yes		71.9	25	72.8	23
VS_0633	*yrbS/acp*	Sodium/proton-dependent alanine carrier protein	IM			6.2	4	10.5	6
VS_0685	*ompK*	Outer membrane protein K	OM	yes		53.8	12	38.5	9
VS_0766		Putative oligogalacturonate-specific porin, KdgM	OM	yes		22.8	4	16.5	3
VS_0861		Putative long-chain fatty acid transport protein	OM	yes		67.0	20	59.5	17
VS_0990	*oppA*	Periplasmic oligopeptide-binding protein	Periplasmic	yes		58.9	28	50.0	18
VS_1055	*argT*	Lysine-arginine-ornithine-binding periplasmic protein precursor, abc transporter	Periplasmic	yes		77.3	16	75.4	15
VS_1068		Putative porin	OM	yes		72.4	22	65.5	21
VS_1116	*tolB*	Translocation protein tolB	Sec exported	yes		58.1	25	39.7	14
VS_1118	*ybgF*	Putative tol-pal system protein YbgF	OM	yes		60.4	13	36.6	9
VS_1121	*viuA*	TonB-dependent Vibriobactin receptor	OM			64.1	33	61.2	34
VS_1300		Putative outer membrane efflux protein TolC	OM	yes		12.3	4	18.3	6
VS_1393		putative Type I secretion outer membrane protein, TolC	OM	yes		44.1	18	62.7	22
VS_1403	*aapJ*	General L-amino acid-binding periplasmic protein aapJ	Periplasmic	yes		57.0	17	57.0	16
VS_1521	*sypC*	Putative Periplasmic protein SypC involved in polysaccharide export	OM	yes		9.2	5	9.9	6
VS_1627		Beta-barrel outer membrane protein (OmpA-like)	OM	yes		21.3	3	28.4	4
VS_1633	*cirA / irgA*	Iron-regulated outer membrane virulence protein	OM	yes		49.4	25	45.3	26
VS_1774		Beta-barrel outer membrane protein (OmpA-like)	OM	yes		29.9	4	29.9	4
VS_1799		Beta-barrel outer membrane protein (OmpA-like)	OM	yes		17.8	3	14.4	3
VS_1820		Beta-barrel outer membrane protein (OmpA-like)	OM	yes		41.6	8	41.2	8
VS_1843		Putative Type I secretion outer membrane protein, TolC	OM	yes		64.9	21	62.6	19

VS_2109	*blc*	Bacterial lipocalin blc precursor (outer membrane lipoprotein)	OM (lipo)	yes	31.3	5	31.3	5
VS_2116	*iutA*	TonB-dependent Ferric aerobactin receptor	OM	yes	48.1	28	34.9	20
VS_2212		TRAP-type C4-dicarboxylate transport system, periplasmic component	Periplasmic	yes	45.8	13	34.8	8
VS_2285	*chiP*	Putative chitoporin	OM	yes	41.4	12	42.4	12
VS_2343	*ompH / skp*	Outer membrane chaperone Skp (OmpH)	Periplasmic	yes	29.7	5	20.3	3
VS_2395	*btuA*	Putative tonB dependent receptor	OM	yes	45.5	25	18.3	9
VS_2443	*cpaC*	Putative type II/IV secretion system secretin RcpA/CpaC, associated with Flp pilus assembly	Sec exported	yes	22.1	9	24.0	7
VS_2494	*ompU*	Outer membrane protein, OmpU	OM	yes	51.4	18	51.4	18
VS_2518	*fbpA*	Iron(III) ABC transporter, periplasmic iron-compound-binding protein	Periplasmic	yes	37.9	9	32.4	7
VS_2998	*btuB*	Outer membrane vitamin b12 receptor	OM	yes	49.3	22	48.1	21
VS_3101	*sufI*	Putative Mn2+ multicopper oxidase	Periplasmic	yes	10.8	4		
VS_II0158	*lamB*	Putative maltoporin	OM	yes	39.9	14	23.5	8
VS_II0159	*malM*	Putative maltose operon periplasmic protein	OM (lipo)	yes	55.9	11	30.7	5
VS_II0220	*malE*	Maltose-binding periplasmic protein	Periplasmic	yes	42.3	11	11.7	3
VS_II0310	*ompC*	Outer membrane protein OmpC	OM	yes	88.2	31	32.4	7
VS_II0361	*ompN*	Outer membrane protein OmpN	OM	yes	39.8	12	50.0	12
VS_II0395	*ompA*	Outer membrane protein OmpA	OM	yes	53.0	18	57.2	16
VS_II0501	*tonB*	Putative ferrioxamine B receptor	OM	yes	44.7	19	35.4	16
VS_II0529	*vctA*	Putative enterobactin receptor VctA	OM	yes	24.3	12	22.7	10
VS_II0677	*fhuA*	Putative TonB dependent ferrichrome-iron receptor	OM	yes	63.6	42	50.3	32
VS_II0738	*traF*	putative TraF-related protein	OM	yes	47.6	14	30.7	9
VS_II0751	*hutA*	Putative TonB-dependent heme and hemoglobin receptor HutA	OM	yes	73.3	56	69.0	46
VS_II0773		Long-chain fatty acid transport protein	OM (lipo)	yes	26.6	8	23.7	7
VS_II0860		Putative outer membrane efflux protein	OM	yes	18.1	6	18.7	7
VS_II0866		Putative permease	OM	yes	22.7	6	22.4	5
VS_II0987	*vasD*	Putative Type VI secretion lipoprotein/VasD	OM (lipo)	yes	48.0	8	25.7	4
VS_II1127	*pvuA (fecA)*	Fe(3+) dicitrate transport protein FecA	OM	yes	78.1	44	76.3	43
VS_II1128	*psuA*	Putative ferric siderophore receptor PsuA	OM	yes	67.2	44	65.4	36
Cell motility								
VS_0803	*flgD*	Flagellar hook capping protein FlgD	Extracellular		29.2	6	16.8	3
VS_0804	*flgE*	Flagellar hook protein flgE	Extracellular		24.0	5	30.0	7
VS_0810	*flgK*	Flagellar hook-associated protein FlgK	Extracellular		10.8	5	19.0	8
VS_0812	*flaA*	Flagellin core protein A	Extracellular		49.9	13	78.9	24
VS_0813	*flaB*	Polar flagellin B	Extracellular		45.2	11	81.6	35
VS_0814	*flaC*	Flagellin C	Extracellular		33.2	9	87.5	33
VS_0816	*flaH / fliD*	Flagellar hook-associated protein FlaH	Extracellular		5.7	3	5.9	3

VS_0828	*fliK*	Polar flagellar hook-length control protein FliK	Extracellular		26.4	10	9.6	3
VS_2293	*flaD*	Polar flagellin B/D, FlaD	Extracellular		46.7	12	86.5	36
Cell wall/membrane/envelope biogenesis								
VS_0078		Putative Sporulation/cell division region protein	Periplasmic	yes	11.5	3	11.5	3
VS_0209	*wbfD*	Putative WbfD protein	OM (lipo)	yes	23.4	4	14.2	3
VS_0212	*wbfB*	Putative WbfB protein	OM	yes	43.5	23	24.8	12
VS_0439	*lppC/lpoA*	Putative lipoprotein LpoA, activator of penicillin binding protein 1A	OM (lipo)	yes	65.1	31	54.3	21
VS_0559	*yfiO/BamD*	Outer membrane protein assembly complex subunit YfiO (YaeT complex)	OM (lipo)	yes	29.4	8	27.8	8
VS_0622	*yfgL/BamD/BamB*	Outer membrane protein assembly complex subunit YfgL (YaeT complex)	OM (lipo)	yes	45.1	12	29.3	8
VS_0690		Putative lipoprotein	OM (lipo)	yes	52.1	7	70.1	8
VS_0717	*lptE*	Luciferase, Rare lipoprotein B involved in LPS assembly (LptE superfamily)	OM (lipo)	yes	76.5	13	46.2	8
VS_1078	*slyB*	Putative outer membrane lipoprotein SlyB	Sec exported	yes	28.7	4	21.3	3
VS_1209		Outer membrane yesprotein (OmpA_C-like superfamily)	OM (lipo)	yes	50.5	6	36.5	6
VS_1776	*mipA*	MltA-interacting protein MipA	OM	yes	11.8	4	13.5	4
VS_1844		Putative outer membrane protein, OmpA family	OM (lipo)	yes	53.5	8	37.7	6
VS_2222	*slp*	Putative Starvation lipoprotein Slp paralog	OM (lipo)	yes	67.4	8	28.9	4
VS_2304	*bamC*	Outer membrane protein assembly factor BamC	OM (lipo)	yes	36.2	10	27.6	8
VS_2344	*yaeT*	Outer membrane protein assembly complex subunit YaeT (YaeT complex)	OM	yes	42.1	26	39.0	25
VS_2477	*nlpI*	Lipoprotein, NlpI	OM (lipo)	yes	21.2	6	26.5	7
VS_3040		Membrane protein	OM (lipo)	yes	18.8	7	15.9	6
VS_II0199	*lpp*	Major outer membrane lipoprotein precursor (Murein-lipoprotein)	OM (lipo)	yes	33.6	7	33.6	8
Energy/Respiration								
VS_2589	*cymA*	Putative exported protein, putative porin (CymA protein precursor)	OM	yes	20.0	6	18.3	6
VS_II0747	*damX*	Putative cytochrome C biogenesis protein CcdA / DamX-related protein	OM (lipo)	yes	50.8	8	58.7	9
Translation								
VS_3141		Translation elongation factor activity	OM	yes	36.8	9	18.9	6
Proteins of unknown functions								
VS_0240		Uncharacterized low-complexity protein	Sec exported	yes	54.6	5	54.6	5
VS_0788		Conserved lipoprotein of unknown function	Unknown		32.7	3	30.0	3
VS_0927		Putative iron-regulated protein	OM (lipo)	yes	30.8	9	22.5	5
VS_1146		Conserved lipoprotein of unknown function	OM (lipo)	yes	37.5	3	37.5	3

VS_1427		Large exoproteins involved in heme utilization or adhesion	Sec exported	yes	51.1	25	45.5	18
VS_1828		Conserved exported protein of unknown function	Sec exported	yes	47.8	7	47.8	7
VS_2070		Conserved exported protein of unknown function	Sec exported	yes	23.8	5	16.2	3
VS_2076	*ycfM*	Outer membrane lipoprotein YcfM	OM (lipo)	yes	54.0	9	55.1	10
VS_2077	*ycfL*	Periplasmic lipoprotein YcfL	OM (lipo)	yes	41.2	5	37.4	4
VS_2078	*ybbK*	Conserved lipoprotein with TPR repeats	OM (lipo)	yes	36.5	11	26.7	8
VS_2315		Conserved protein of unknown function	Sec exported	yes	37.5	14	29.2	11
VS_2372		Conserved lipoprotein of unknown function	OM (lipo)	yes	55.4	6	55.4	6
VS_II0865		Conserved protein of unknown function	Sec exported	yes	32.9	3	31.1	3
VS_II0989		Conserved protein of unknown function	OM	yes	32.5	5	20.7	4
VS_II1101		Putative uncharacterized protein	OM (lipo)	yes	41.5	19	56.4	25

Table S2. Molecular functions associated to OMV proteins.

Two independent OMV preparations were compared: OMV prep #1 was crude while the OMV prep #2 was purified on density gradient. The numbers of proteins assigned to a given molecular function are similar in both preparations. The molecular functions associated to the 132 proteins common to OMV prep #1 and #2 (detailed in Table S1) are shown on the right column.

	OMV prep #1 (crude)		OMV prep #2 (purified on density gradient)		Proteins common to OMV #1 and #2	
Molecular function	**number of proteins**	**%**	**number of proteins**	**%**	**number of proteins**	**%**
Enzyme activity	56	29.8	49	27.7	33	25.0
Transport/Conjugation	75	39.9	61	34.5	54	40.9
Cell motility	10	5.3	10	5.6	9	6.8
Cell wall/membrane/envelope biogenesis	18	9.6	25	14.1	18	13.6
Energy/Respiration	3	1.6	4	2.3	2	1.5
Stress response	2	1.1	0	0	0	0
Translation	3	1.6	4	2.3	1	0.8
Proteins of unknown functions	21	11.2	24	13.6	15	11.4
Total proteins	**188**		**177**		**132**	

Table S3. Strains, plasmids and oligonucleotides.

	Description/sequence	Reference
Bacterial strain		
LGP32	*V. tasmaniensis (Splendidus clade)*	(Gay et al., 2004)
Δvsm	LGP32 *Δvsm* (VS_1267, M4 metalloprotease)	(Le Roux et al., 2007)
Δvsp	LGP32 *Δvsp* (VS_II0815, intravesicular serine protease)	This study
π3813	*E. coli*, *lacIQ, thi1, supE44, endA1, recA1, hsdR17, gyrA462, zei298::Tn10* [Tc^R] *ΔthyA::(erm-pir116)* [Erm^R]	(Le Roux et al., 2007)
β3914	*E. coli* (F^-) RP4-2-Tc::Mu ΔdapA ::(erm-pir) [Km^R Em^R] *zei298*:*Tn*10	(Le Roux et al., 2007)
Plasmids		
pSW7848	$oriV_{R6Kγ}$; $oriT_{RP4}$; *ara*C-P_{BAD}*ccdB*	(Le Roux et al., 2007)
Oligonucleotides		
281112-1	5'-ATGAATGTTAACCATACAATGAGTCC-3'	This study
281112-2	5'-ACAGGGTGTTTAACGTAATGAGATAACTCCTTGTAACCCC-3'	This study
281112-3	5'-GGGGTTACAAGGAGTTATCTCATTACGTTAAACACCCTGT-3'	This study
281112-4	5'-TGGACTTTTACACTTACAACGG-3'	This study
VS_II0815-Fw2	5’- CGCTGAAGTTCGTGGTAAG -3’	This study
VS_II0815-Rv2	5’- TTGTGACATAAGCACCTCCA -3’	This study